

University of Mississippi

eGrove

Honors Theses

Honors College (Sally McDonnell Barksdale
Honors College)

2004

Spatial Variability of Soil Electrical Conductivity and its Response to Soil Physical Properties

Matthew David Sleep

Follow this and additional works at: https://egrove.olemiss.edu/hon_thesis

Recommended Citation

Sleep, Matthew David, "Spatial Variability of Soil Electrical Conductivity and its Response to Soil Physical Properties" (2004). *Honors Theses*. 2262.

https://egrove.olemiss.edu/hon_thesis/2262

This Undergraduate Thesis is brought to you for free and open access by the Honors College (Sally McDonnell Barksdale Honors College) at eGrove. It has been accepted for inclusion in Honors Theses by an authorized administrator of eGrove. For more information, please contact egrove@olemiss.edu.

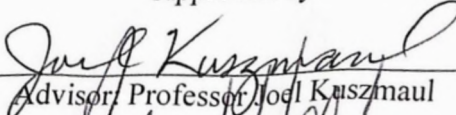
SPATIAL VARIABILITY OF SOIL ELECTRICAL CONDUCTIVITY AND ITS
RESPONSE TO SOIL PHYSICAL PROPERTIES

By
Matthew David Sleep

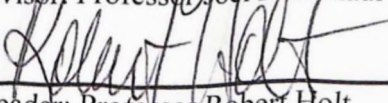
A thesis submitted to the faculty of The University of Mississippi in partial fulfillment of
the requirements of the Sally McDonnell Barksdale Honors College.

Oxford
December 2004

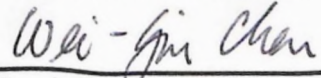
Approved by



Advisor: Professor Joel Kuszmaul



Reader: Professor Robert Holt



Reader: Professor Wei-Yin Chen

ACKNOWLEDGEMENTS

Whole heartedly I thank Dr. Robert Holt and Dr. Joel Kuszmaul. Their trust in my abilities as a student and guidance through not only this thesis, but my college career are the greatest honors I have ever received. Their constant focus on students and teaching make them the most valuable assets to The University of Mississippi. I hope to one day be as thoughtful and dedicated as they are.

I also wish to acknowledge the Geological Engineering Senior Design Class of 2004. If all of my future coworkers are like them, my career will be blissful. Lucky Pierre will forever be etched into the memory of the five men in GE 490.

The Sally McDonnell Barksdale Honors College at the University of Mississippi has become an amazing institution. I acknowledge their guidance with this thesis, for creating a great program, and employing me for two years. If the paper in the computer lab is ever low, do not hesitate to call.

ABSTRACT

MATTHEW DAVID SLEEP: Spatial Variability of Soil Electrical Conductivity and Its Response to Soil Physical Properties
(Under the direction of Robert Holt and Joel Kuszmaul)

The Soil Moisture Observatory (SMO) at the University of Mississippi (UM) is a 5 acre tract of a former agricultural field at the UM Biological Field Station. Preliminary investigations of this site included 60 continuous soil cores using the Geoprobe sampling technique. These soil cores were taken to a depth of 1.5 meters to correspond to the approximate depth of penetration for a Geonics EM38. The Geonics EM38 uses electromagnetic induction to measure apparent electrical conductivity of the soil. After three weekly measurement episodes using the EM38, the soil samples were taken. These samples were analyzed for particle size distribution, porosity, bulk density, iron content, and moisture content. Little direct correlation exists between the EM38 response and these measured soil properties. The temporal variations of the variograms of EC indicate a complex relationship between soil properties and EC.

TABLE OF CONTENTS

LIST OF FIGURES.....	v
LIST OF TABLES.....	vi
1.0 INTRODUCTION.....	1
1.1 FIELD SITE.....	3
1.2 METHODS AND MATERIALS.....	8
1.3 DATA ANALYSIS.....	15
2.0 RESULTS AND DISCUSSION.....	17
2.1 CORRELATION OF EM38 AND VOLUMETRIC MOISTURE CONTENT.....	17
2.2 ANALYSIS OF THE VERTICAL AND HORIZONTAL DIPOLE MODES.....	21
2.3 REGRESSION ANALYSIS OF SOIL PROPERTIES.....	24
2.4 VARIABILITY OF EC _a REFLECTED BY VARIOGRAMS.....	26
2.5 NEGATIVE CORRELATION FOUND IN T LINE.....	31
3.0 CONCLUSIONS.....	34
BIBLIOGRAPHY.....	35
APPENDIX A.....	38

LIST OF FIGURES

Figure 1	Location Map of the University of Mississippi Biological Field Station.....	3
Figure 2	Generalized Site Specific Stratigraphic Column.....	5
Figure 3	Map of EM Sampling Locations at UMBFS.....	10
Figure 4	Soil Type by Grain Size.....	13
Figure 5	Linear Regression of VMC and EC_H	19
Figure 6	Linear Regression of VMC and EC_V	20
Figure 7	Linear Regression of EC_H and EC_V	22
Figure 8	Average Volumetric Moisture Content from Each Sample.....	23
Figure 9	Significant Precipitation Events during Sampling.....	27
Figure 10	Variogram of the E_{Ca} along the T-line in the Horizontal Dipole Mode.....	28
Figure 11	Variogram of the E_{Ca} along the T-line in the Vertical Dipole Mode.....	29

LIST OF TABLES

Table 1	Depth Contributions to the Readings of an EM38 Meter.....	8
Table 2	Correlation Coefficients of Soil Properties and ECa.....	17
Table 3	Regression Modeling Analysis Results.....	25
Table 4	Correlation Coefficients of ECa and Volumetric Moisture Content.....	31

1.0 Introduction

Recently electromagnetic inductance techniques have gained popularity for their ease of use, and relative inexpensiveness. Electromagnetic induction is used for soil moisture content measurement, soil salinity determinations, and groundwater contamination. Moisture of near surface soils greatly influences the agricultural productivity of a soil (Schlesinger et al. 1990) and a host of other hydrogeological processes. A soil's moisture will also affect infiltration, flooding, erosion, and performance of engineered covers (Reedy and Scanlon 2003). Soil salinity significantly influences agricultural processes. A quick and non-invasive measurement of soil moisture and salinity is very useful for assessing these items.

Several authors have proposed that apparent electrical conductivity (ECa) measurements can be used to estimate soil salinity (Rhoades et al. 1990; Lesch et al. 1995; McKenzie et al. 1997; Herrero et al. 2003). Others have proposed that soil water content can be monitored using electromagnetic inductance (Sheets and Hendrickx 1995; Reedy and Scanlon 2003). Sheets and Hendrickx (1995) used 65 neutron probe access tubes to monitor soil moisture content and a Geonics EM31 to measure ECa. In an arid environment they found a linear regression model best describes the relation between water content and ECa with an R^2 for the single model of 0.64. A similar method of using neutron probe access tubes for water content measurement and studying the relation to electromagnetic inductance measurements was performed in a more humid environment with few dissolved electrolytes (Kachanoski et al. 1990). Approximately 80% of the variation in soil water content was explained by the ECa measurement. A recent study related soil

water content to ECa in an engineered fill (Reedy and Scanlon 2003). R^2 values of 0.96 were produced for soil water content in both the first 0.75m of soil and 1.5m of soil and the measured ECa value.

The purpose of this research is to determine if a relation exists between soil water content and ECa measurements using an EM38 in sandy Northern Mississippi soils that are nearly or completely saturated. This study differs from previous studies because measurements of soil electrical conductivity taken with the EM38 were compared to physical volumetric moisture content measurements from extracted soil cores rather than other non-invasive methods such as neutron probe measurements. It is anticipated that a relation exists with apparent electrical conductivity of the soils increasing with increased soil water content.

The research included monitoring of a field site over several weeks using the Geonics EM38 to measure the apparent electrical conductivity of the underlying soil. After three weeks of monitoring, soil cores were extracted at each point where the EM38 took measurements. These soil cores were analyzed for soil moisture content, soil chemistry, and grain size. These soil properties were compared to the electrical conductivity measurements obtained from the EM38.

1.1 Field Site

The study site for this investigation is a former agricultural field at the University of Mississippi (UM) Biological Field Station (BFS) known as the University of Mississippi Soil Moisture Observatory (SMO). The location of the Biological Field Station is shown in Figure 1.

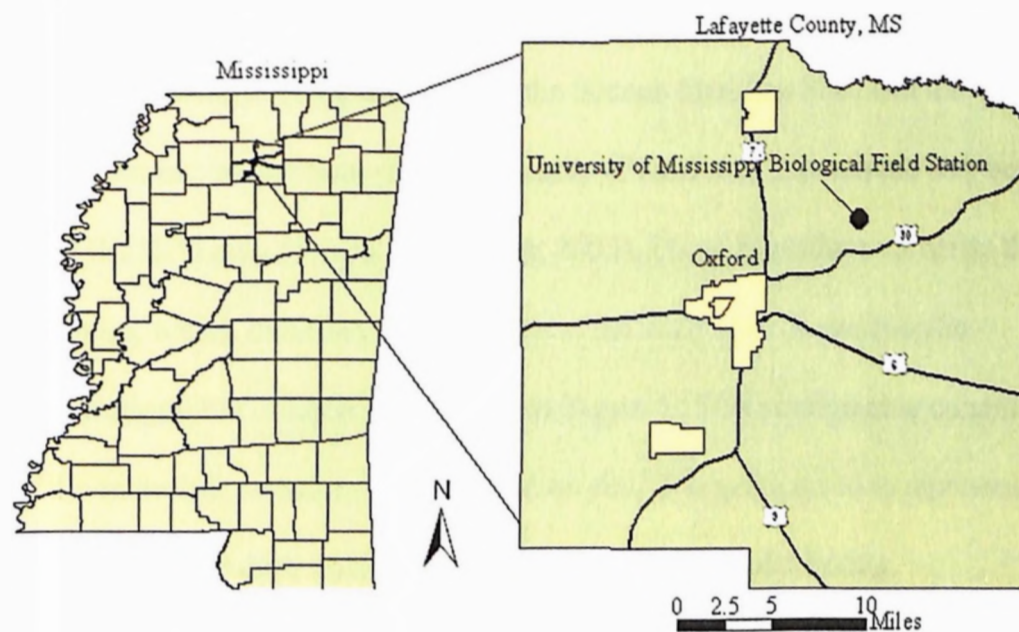


Figure 1 Location Map of University of Mississippi Biological Field Station

The BFS is located 11 miles from the UM campus in Oxford, Mississippi. The BFS is within the headwaters of the Little Tallahatchie River, which is a tributary of the Yazoo River. The BFS began as a fish farm in 1947, known as Ole Miss Fisheries Inc. The fishery was later known as Minnows Incorporated, operated by Herbert Kohn Corp out of Memphis, Tennessee. Weyerhaeuser Corporation purchased the land in the early 1980's. In 1986 The University of Mississippi purchased the property from Weyerhaeuser Corporation with an additional 500 acres donated to the University of Mississippi for research and educational purposes.

Additional land was purchased in 1989 and 1996 which brought the BFS to its current total acreage of 740 acres.

The study site is located on the Bagley Lake (1980) quadrangle. The site is a former agricultural field currently covered with tall grasses. Trees surround the field on the north, east, and west borders. The south boundary is a dirt and gravel road. A decrease in elevation is found at the northern end of the site.

The BFS is within the outcrop belt of the Eocene Meridian Sand and the Tallahatta Formation, which both consist primarily of sand with subordinate clay beds and lenses in the BFS area (Swann and Lutken, 2002). These formations comprise the Claiborne Group, which outcrops at the surface of the study site. A site specific generalized stratigraphic column is presented as Figure 2. This stratigraphic column represents the materials found at our investigation site. It is generalized to represent the entire study site and does not reflect the findings of a particular boring.

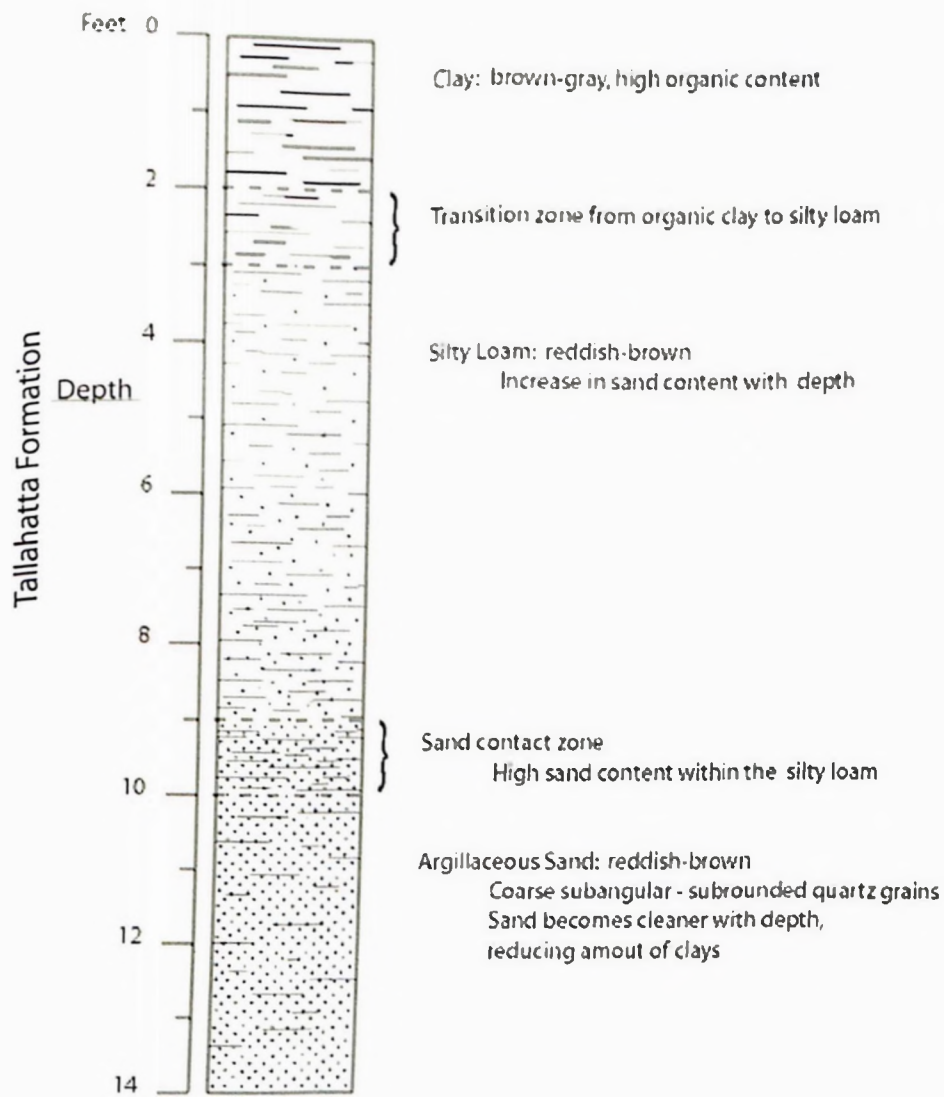


Figure 2 Generalized Site Specific Stratigraphic Column

The Meridian Formation is predominantly white sand in the upper portion and grades downward into rusty brown or red sand, which is cross-bedded to evenly stratified with light-colored sand (Attaya 1951). The Meridian Sand is an extremely well-sorted, medium sand throughout its entire thickness. The unit is uniform throughout its thickness, except for minor areas of fine and coarse grain sands. The lower portion of the Meridian is a coarse subangular to well-rounded sand with pebbles. Mica is the most common accessory mineral in the quartz sand. This portion has a more red color from iron oxidation.

The Tallahatta Formation in the Lafayette County area is a mix of sands, clays, clay shale, and siltstone (Attaya 1951). Subdivision of the differing materials is difficult. Sand makes up a majority of the formation and the clays, shales, and siltstones are local developments within the sand. The lower beds are mainly fine-grained sands.

This silt is part of a broad band of silty loess deposited during the late Pleistocene to early Recent periods along the lower Mississippian Valley (Krinitzsky 1967). This silt began as glacial flour that was carried away from the glacier via a braided stream and was then wind blown and redeposited. In the area of northern Mississippi, the silt deposited within five to fifteen miles of the Mississippi River is very calcareous. This is because the deposition near the Mississippi River was rapid and the silt was buried before the calcareous cement could be weathered. At the field site, the calcareous cement of the silt has been weathered and the material is referred to as 'Brown Loam' (Krinitzsky 1967). The brown coloring is a result of iron salts weathering out of dark minerals such as hornblende and pyroxene. The mineral composition of these silts is predominately quartz with minor feldspars and some clay. The clay minerals constitute thirteen to thirty percent of the 'brown loam' composition (Krinitzsky 1967). Thin sections of these silts have shown that the porosity ranges from 43-54%. Also the clay is evenly distributed in the brown loam thoroughly surrounding the silt particles with clay (Krinitzsky 1967).

The most accessible groundwater source (aquifer) at the BFS is the Meridian Sand, but there are deeper and less productive aquifers in the vicinity (Swann and Lutkin 2002). Locally the Meridian Sand maybe adjacent to older sands of the

Wilcox Group, which allows water movement between the two. Since the Meridian and Tallahatta consist of sands, movement of water occurs between these two as well. This aquifer is officially known as the Meridian Upper Wilcox Aquifer; locally it is referred to as the Tallahatta-Meridian-Upper Wilcox Aquifer.

In the upland areas of the BFS only sand is found between the surface and the water table (Swann and Lutkin 2002). The equipotential surface is often the same as surface topography for the unconfined aquifer in these locations. In some areas fine grain sediments confine the groundwater movement. A recent well installation adjacent to the field site indicated the water table was 52 feet below the surface. The water table had no influence on this investigation because the lower limit of soils investigated was 1.5 meters.

1.2 Methods and Materials

A total of 60 sample sites were used for this field study. Data collection began with ECa measurements from the Geonics EM38. The EM38 obtains the apparent soil electrical conductivity by measuring a magnetic field in the soil induced by the instrument. A transmitting coil inside the instrument generates a primary magnetic field which causes electric current to be induced within the earth. Then another coil inside the instrument receives the secondary magnetic field created by the induced subsurface current flow. The measured electromagnetic field is used to interpret apparent electrical conductivity (ECa) of the soil. The EM38 measures apparent electrical conductivity of the soil in two different modes, a vertical dipole and horizontal dipole mode. The difference between these two modes is depth of measurement. Table 1 (McKenzie et al. 1997) indicates the depth contributions of the soil toward the EM38 meter reading.

Depth (cm)	Horizontal Mode	Vertical Mode
0-30	0.43	0.14
30-60	0.21	0.22
60-90	0.10	0.15
90-120	0.06	0.11
120-150	--	0.08
150-180	--	0.03
Sum	0.80	0.73

Table 1 Depth Contributions to the Readings of an EM 38 Meter

The sums are not completely equal to one because theoretically the induced electrical current is infinite in depth but for measurement purposes, it is given a lower limit.

In the horizontal dipole mode the EM38 reads ECa at a shallower depth than the vertical dipole mode. In the horizontal dipole mode the EM38 has an effective depth of 0.75m and 1.5m in the vertical dipole mode. Before each measurement day, the EM38 was calibrated using the Geonics Limited EM38 Ground Conductivity Meter Operating Manual 2002. Measurements were taken on weekly intervals for four weeks. The dates of measurements were October 16, 23, 30, and November 6, 2003.

On the third day of EM38 measurements, soil samples were taken. A Geoprobe 5400 was used to extract soil samples from the 60 EM measurement sites. Figure 3 is a map of the sampling locations.

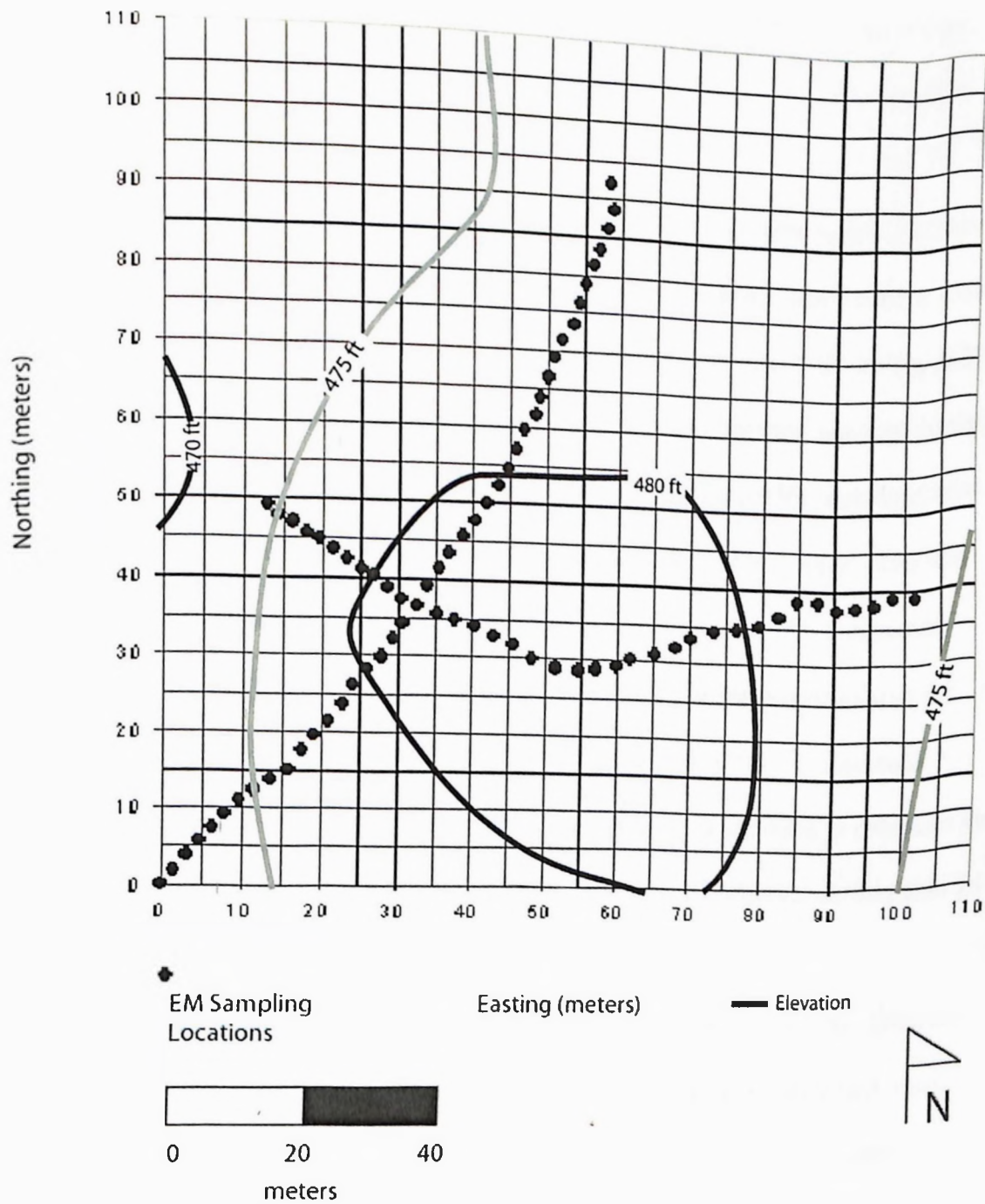


Figure 3 Map of EM Sampling Locations at UMBFS.

The sampling sites were split into north-south and east-west transects. The east-west transect is referenced as the T-line. The north-south transect is referenced as the HR-line. Each sample site was approximately 1m apart. The soil samples were taken as

continuous cores to a depth of 1.5m to correspond to the penetration depth of the EM38 meter. Samples were extracted in Lexan liners and capped to preserve the field moisture content.

The samples were analyzed for volumetric moisture content within 36 hours after extraction from the field site. Once in the lab, the 1.5m soil cores were divided into five samples. Samples were taken at the following intervals: 0.09-0.18m, 0.33-0.42m, 0.58-0.67m, 0.82-0.91m, 1.06-1.15m. By taking volumetric moisture content measurements in intervals, we were able to create a moisture profile with depth and also create an average soil moisture content over the entire depth. Volumetric soil moisture was obtained by calculating the volume of the sample. The Geoprobe process created uniform cylindrical soil samples. Each sample was measured for diameter and length using calipers three times in each orientation. An average diameter and length was obtained from these measurements and used to calculate the volume of the sample. The sample was then oven dried for a period no less than 24 hours to obtain the volumetric moisture content.

To further study the relationship between ECa and soil properties, grain size analysis was also performed on the 60 samples. All five samples from each sampling site were placed in a soil pulverizer. The sample was run through the pulverizer twice to obtain a composite sample. Of the composite sample, 250 grams were separated to be used for grain size analysis. Samples were placed in a No. 200 sieve and separated into fine and coarse grained material according to ASTM Standard D6913-04. After this sieving the percentage of sand sized particles for each composite sample was known.

A Beckman Coulter LS 13 320 Particle Size Analyzer was used for differentiating between clay and silt sized particles. The instrument is primarily used for pharmaceutical purposes but can be used on any sample between 0.4 and 2000 microns. Laser diffraction was used on the sample that passed the No. 200 sieve. Before beginning the process, a standard operating procedure was created for consistency in measurements. Before each sample was loaded into the machine, background noise from the laser was measured, offsets were measured, and the laser was aligned. The samples were mixed in the sample bags to ensure a homogeneous sample and then added to the unit until an obscuration of 10% was reached \pm 3%. If obscuration was greater than 13%, the sample was flushed from the system and the process repeated. Output from the particle size analyzer consisted of a data file with percent of sample above and below 2 microns recorded. This data combined with the sieve data gave a particle size distribution of each sample in terms of sand, silt, and clay. Figure 4 displays the results of the grain size analysis. Highlighted in yellow are the limits of 'Brown Loam' materials explored by Krinitzsky. Also the T Line is divided into sample number by groups of ten. Sample 1 is the southernmost sample with sample numbers increasing to the north to sample 40. Observed is a general decrease in sand content to sample 20, then a general increase in sand content to sample 40. This follows the topography of our sample site. There is less sand present in the areas with the higher topography and more sand as the samples move topographically down from the top of the hill.

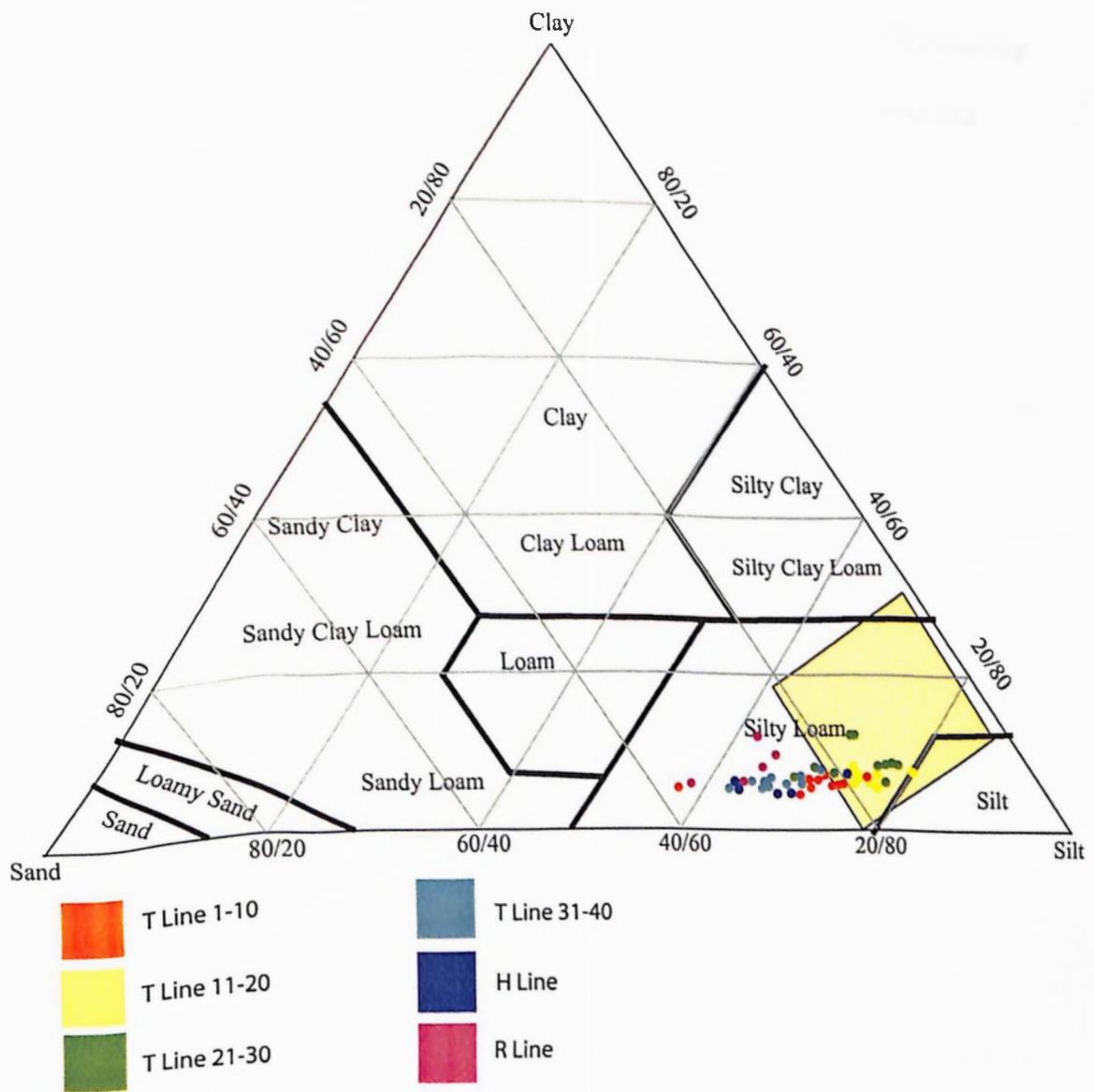


Figure 4 Results of Grain Size Analysis

The composite soil samples also were also analyzed for soil chemistry. Of the composite sample, 50 grams was used for soil digestions. Digestions were performed by heating a solution of nitric acid together with the sample. The process was repeated using a solution of hydrochloric acid. The solution was then placed into an Inductively Coupled Plasma Atomic Emission Spectrometer. This spectrometer determined the elemental composition of the sample in terms of Ca, Fe, Al, K, Mn, Mg, and Na. Of particular interest was the presence of Fe. The magnetic properties

of the Fe might interfere with the accuracy of the EM38. High levels of Fe and Mg will generate an outside signal that alters the readings of the EM38 (Sheets and Hendrickx 1995).

1.3 Data Analysis

Data sets of EM38 measurements, volumetric soil water contents, grain size distributions, and soil digestions were available for investigation. ECa can vary greatly due to changes in soil temperature (Slavich and Petterson 1990). Therefore it is necessary to convert field measured ECa readings to an equivalent reading at 25° C (EC₂₅) using a conversion table given by the U.S. Department of Agriculture (1954). Sheets and Hendrickx fitted a curve to this table to give the following temperature standardization equation:

$$EC_{25} = EC_a * [0.4470 + 1.4034e^{(T/26.815)}]$$

This temperature standardization was applied to all EM38 readings based on temperature information from the BFS weather station.

Study of the ECa given by the EM38 and its relationship to volumetric moisture content was accomplished through correlation tables and linear regressions. ECa measurements were compared to volumetric moisture content from each sample depth as well as an average soil moisture content measurement. After correlations and linear regressions using volumetric moisture content and ECa, the ECa was compared to clay content and the soil chemistry using these same techniques.

Spatial variations in ECa and soil physical properties were studied using variograms. Variograms relate measurements to one another spatially. The equation for a variograms is:

$$\gamma(h) = \frac{1}{2N} \sum_{i=1}^N (f_{1i} - f_{2i})^2$$

Where N is the number of is the number of pairs of points whose separation distance falls within the lag interval and f_{1i} and f_{2i} are the values at the head and tail of each

pair of points. The head and tail are the values compared at a separation distance of h . The main structural parameters from a variograms that relate to soil moisture are the sill, correlation length, and nugget (Western et al. 1998). Sills represent the total variance of a sample population and can be thought of as the variance between two points. Correlation lengths represent physical distances at which properties no longer become related. A nugget effect is found in samples that are improperly spaced. The term comes from mining practices where there are physical nuggets that represent variations at distances smaller than the compared pairs. Common instances of the nugget effect occurs when samples are placed too far apart and small scale changes in properties are not detected.

2.0 Results and Discussion

2.1 Correlation of EM38 and Volumetric Moisture Content

The data obtained from the field investigation included four dates of EM38 readings, volumetric moisture content measurements, grain size analysis, and soil chemistry information for each measurement site. This data showed complex relationships between soil apparent electrical conductivity and soil properties. Table 2 is a correlation table of the measured soil properties and the apparent electrical conductivity.

Correlation Coefficients						
Variable	T Line		HR Line		Total	
	Vertical ECa	Horizontal ECa	Vertical ECa	Horizontal ECa	Vertical ECa	Horizontal ECa
Porosity	0.31555	0.42509	-0.23508	-0.30007	0.18895	0.17733
Gravimetric Moisture Content	0.02169	-0.34846	-0.10685	-0.01440	-0.05020	-0.21352
Volumetric Moisture Content	-0.17499	-0.55563	-0.02051	0.07836	-0.13456	-0.31190
Bulk Density	-0.31555	-0.42509	0.23508	0.30007	-0.18895	-0.17733
% Sand	0.15405	0.31743	0.03866	0.08727	0.28685	0.11372
% Silt	-0.18579	-0.32919	-0.24038	-0.21889	-0.38790	-0.15622
% Clay	0.03256	-0.13177	0.53020	0.32852	0.26516	0.11630
Fe	0.19921	0.32913	0.36888	0.66900	0.30661	0.43860
Al	0.32425	0.38477	0.17179	0.59717	0.27876	0.44110
Ca	0.30061	0.06529	0.58488	0.20912	0.18712	0.07000
K	0.29853	0.31789	0.14329	0.54632	0.28242	0.37415
Mg	0.09545	0.13351	0.30099	0.45456	0.29695	0.22742
Mn	0.04823	-0.13447	-0.05398	0.18952	0.10281	-0.04930
Na	0.32294	0.14806	0.71147	0.37454	0.50476	0.19225

Table 2 Correlation Coefficients of Soil Properties and ECa

The purpose is to try and identify which soil properties at the University of Mississippi Biological Field Station are controlling the response of the EM38. A high correlation between the gravimetric and volumetric moisture contents was anticipated. Rather than high positive correlations, several negative correlations are observed with moisture content (Table 2). This indicates that something other than moisture content may be controlling the EM38 response. It is possible that the electrical conductivity is more closely related to surface conductivity between clay particles in the soil. The percent clay and ECa have a high correlation along the HR (0.53, 0.33) Line in the vertical dipole mode but is inconsistent with the T Line (0.03,

-0.13) and in the horizontal dipole mode. As mentioned previously, others have reported the EM38 response to be highly dependant on soil salinity. A higher amount of dissolved ions in the soil would increase the electrical conductivity. Moderate correlations exist between ECa and some of the soil chemistry profiles. Particularly the iron, potassium, and sodium have moderate to high correlations with ECa (Table 2). The high correlations are not consistent in every line or dipole mode indicating a highly heterogeneous environment where the EM38 response is controlled by different soil properties depending on the location within the study area. Iron affects the EM38 response differently than the other elements. Because the EM38 uses a magnetic field to measure electrical conductivity, the magnetic field created by high amounts of iron can affect the reading. This is supported by a fairly consistent correlation of iron content and ECa ranging from 0.19 along the T Line in the vertical mode to 0.67 along the HR Line in the horizontal mode.

Interestingly, similar studies performed by others have found higher correlations between moisture content and the ECa. Correlation coefficients of 0.91 for the EC_H and 0.88 for the EC_V modes have been reported (Kachanoski et al. 1988). A predictive model using linear correlation of volumetric moisture content to the EC_H produced an R² value of 0.96 (Reedy and Scanlon 2003). Both of these previous studies used methods such as time domain reflectometry (TDR) or neutron probes to measure the volumetric moisture content. This differs from our study in which physical soil cores were removed and measured for volumetric moisture content. The TDR and neutron probe methods of measuring soil moisture take average moisture content measurements over a larger area when compared to our individual samples.

To further investigate the correlation of the electrical conductivity measured with the EM38 to soil volumetric moisture content, linear regressions were performed. Table 1 indicates the depth contributions to the two modes of the EM38, vertical and horizontal. Because our volumetric moisture content samples were taken at different depths, it is possible to correlate the measurements from the corresponding depths that contribute most to the EM38 measurement. For the horizontal and vertical dipole modes, this is sample depth 1 and the average of sample depths 2 and 3 respectively. Figure 5 is a linear regression of the volumetric moisture content measured from sample depth 1 and the horizontal dipole mode EM38 measurement.

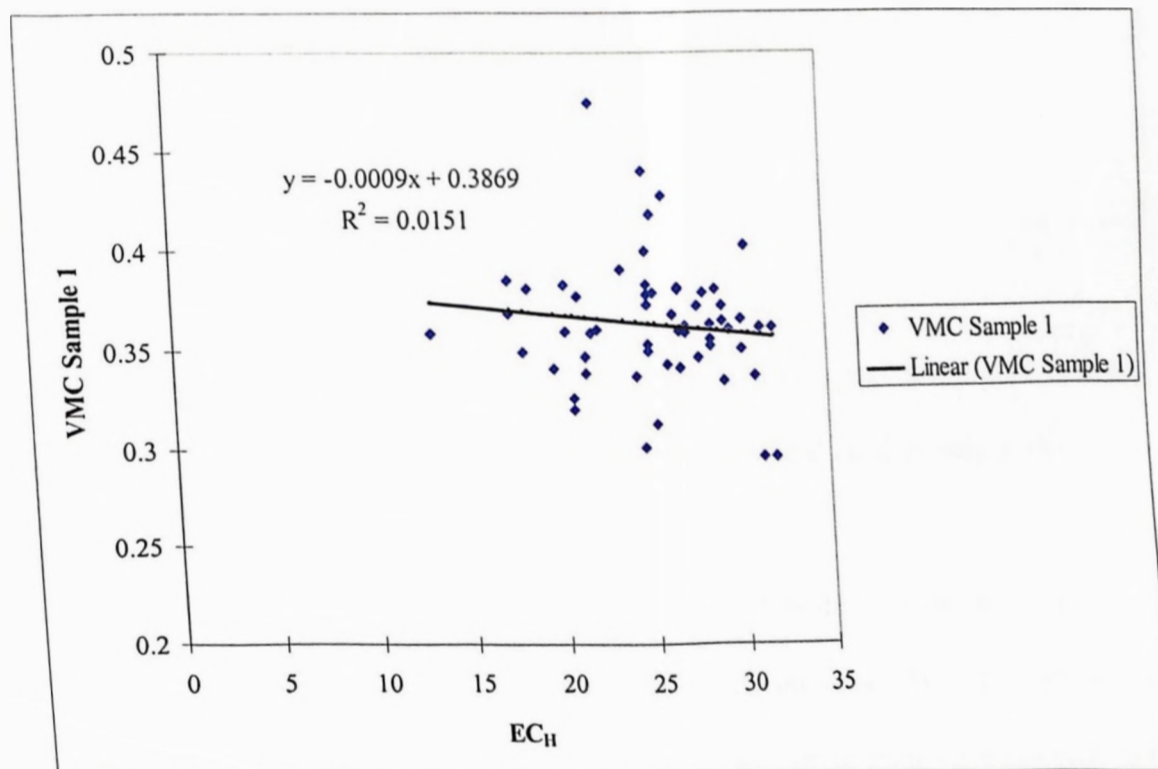


Figure 5 Linear Regression of VMC and EC_H

A non-significant R^2 value of 0.0151 is obtained from the linear regression of the volumetric moisture content and the horizontal mode EM38 reading. This non-

significant R^2 indicates that no linear relation exists between the volumetric moisture content from the soils that influence the response of the EM38 in the horizontal dipole mode. This lack of apparent relation is also observed in the vertical dipole mode (Figure 6).

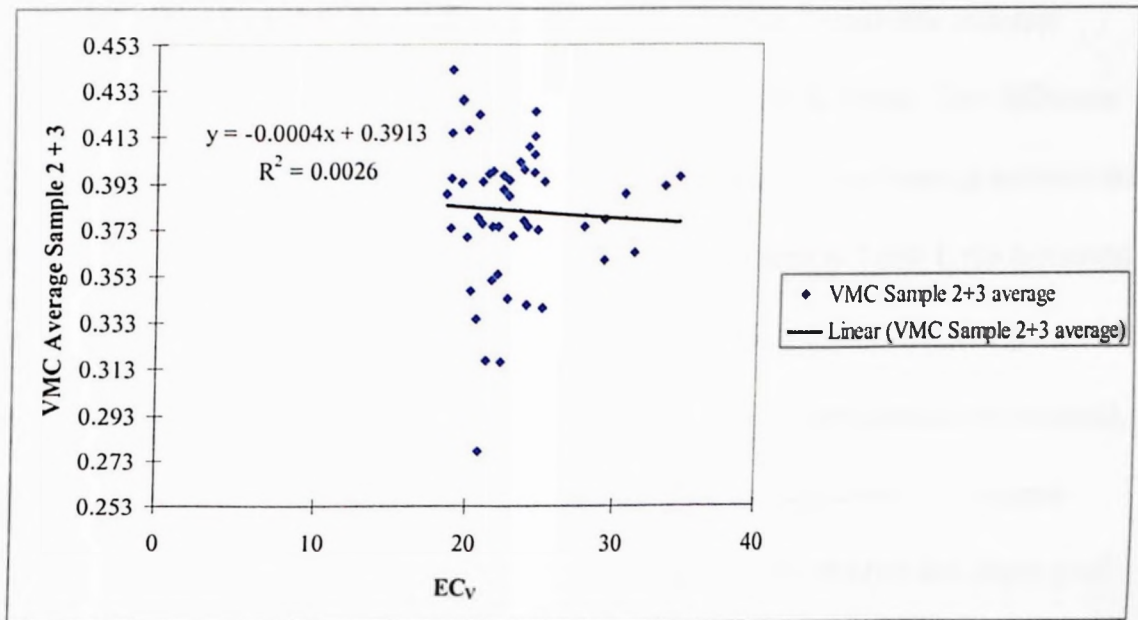


Figure 6 Linear Regression of VMC and EC_v

In the vertical dipole mode, an even smaller level of significance is obtained between the volumetric moisture content and the apparent electrical conductivity in the vertical dipole mode.

This further displays the inability of the EM38 to detect small scale changes in soil moisture content. The samples taken to measure the volumetric moisture content were relatively small ($\sim 75\text{cm}^3$). Changes seen at this small scale were not seen in the EM38 readings. They appeared completely unrelated with R^2 values of 0.0026 and 0.0151. Even when the five samples were averaged to find a single volumetric moisture content measurement for the entire soil core, little correlation was found

(Table 1). At the University of Mississippi Biological Field Station Site there is a complex relationship between apparent electrical conductivity and volumetric moisture content.

2.2 Analysis of the Vertical and Horizontal Dipole Modes

An explanation for the lack of correlation between volumetric moisture content and apparent electrical conductivity is not readily available. One difference between this study and previous studies where a correlation was found is between the horizontal and vertical dipole modes of the EM38. As seen in Table 1, the horizontal mode and vertical mode have different contributions from depth. The vertical mode reaches deeper sediments than the horizontal mode. In a homogeneous environment, these two modes would correlate well. There would be little change in moisture content with depth. This was the case with several previous studies that found good correlation of apparent electrical conductivity and volumetric moisture content. Correlations between EC_H and EC_V with R^2 values of 0.98 and 0.96 (Herrero and Arageus 2003) and 0.83 (Reedy and Scanlon 2003) have been reported. Figure 7 is a linear regression of the EC_V and EC_H measured on the day soil samples were taken.

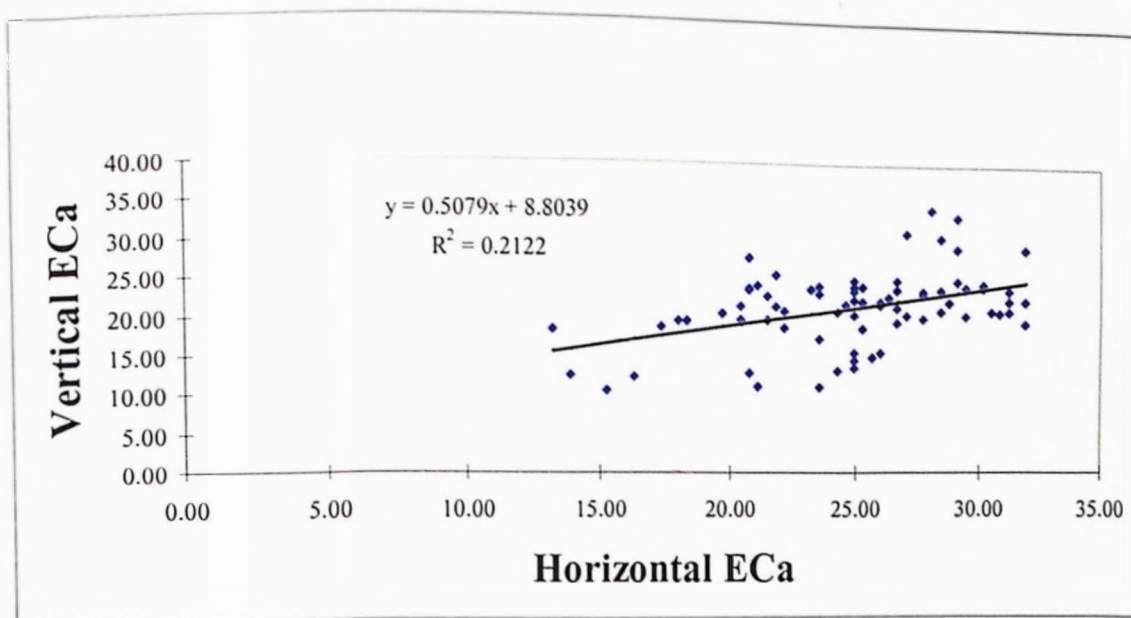


Figure 7 Linear Regression of EC_H and EC_V

From Figure 7 it can be seen that there is some correlation between the vertical and horizontal dipole modes. An R^2 value of 0.21 is obtained between the two modes. This is far less than those obtained from Herrero and Arageus (2003) and Reedy and Scanlon (2003). The low R^2 value suggests that there is significant change in soil properties with depth at the University of Mississippi Biological Field Station causing the vertical and horizontal dipole modes of the EM38 to have little correlation. Figure 8 plots the average volumetric moisture content taken from each sample with depth.

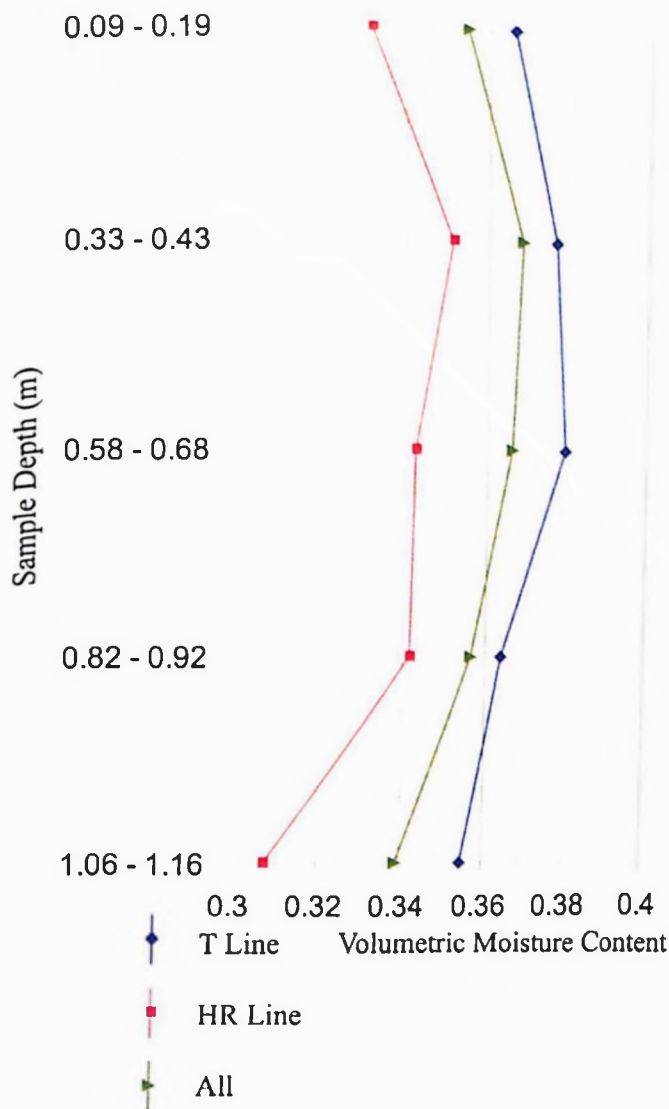


Figure 8 Average Volumetric Moisture Content from Each Sample

Significant differences exist between shallow samples and those deeper. The lack of correlation between the vertical and horizontal dipole modes of the EM38 can partially be explained by this heterogeneity. In the horizontal mode, the EM38 is reading the apparent electrical conductivity of drier soils than the vertical mode. This further illustrates the heterogeneities present at the University of Mississippi Biological Field Station. These heterogeneities might be the cause of the complex relationship between apparent electrical conductivity and volumetric moisture

content. Small scale changes are not reflected in the EM38 measurements but are seen in the volumetric moisture content measurements.

Knowing that significant heterogeneities in soil properties exist at the University of Mississippi Biological Field Station, an attempt was made to define what measured soil properties were influencing the EM38 measurements obtained.

2.3 Regression Analysis of Soil Properties

To determine what soil properties were influencing apparent electrical conductivity of the soil, regression analysis was performed with the dependant variable as the apparent electrical conductivity measured in both the horizontal and vertical dipole direction. Ten measured variables (Fe, Al, K, Na, Mg, Ca, Mn, %Silt, %Clay, and Volumetric Moisture Content) were used in the analysis. The T-line and HR-line have separate regression analyses performed. The best reduced model regression analysis tables are presented in Appendix A. The goal of the regression analysis was to indicate which of the ten variables was significant in predicting the apparent electrical conductivity measured by the EM38. The analysis was run with all ten variables. The multiple linear regression model fitting was performed using a backwards elimination technique. After analysis, the variable with the highest P-value was removed and the analysis was rerun. The variable with the highest P-value has the smallest significance in the predictive model. The process was repeated until the highest coefficient of variation was obtained along with the greatest F statistic to P-value ratio. The results are presented in Table 3.

Multiple Regression Modeling Results					
Population	Dependent Variable	Significant Variables	F Statistic	Model Significance (significance of F statistic)	R ²
HR Line	Horizontal EC	Fe	11.34	0.00460	0.448
	Vertical EC	Fe, Al, K, Na, % Silt, % Clay	12.93	0.00056	0.896
T Line	Horizontal EC	Fe Vol. Moisture Content	10.80	0.00021	0.375
	Vertical EC	K, Mg, Na	3.55	0.02404	0.233

Table 3 Regression Modeling Analysis Results

High R² values were obtained for each mode and line except the T-line in the vertical dipole mode which also had the lowest F statistic value. This indicates that the measured soil physical properties do control the apparent electrical conductivity of the soil at the University of Mississippi Biological Field Station. It is a complex relationship because along each line and with differing modes, separate variables were found to be significant. The only variable found significant repeatedly was iron. This has many implications in using the EM38 as a tool to measure volumetric moisture content of soils. High concentrations of iron and manganese in the soil can generate an outside signal that alters the readings of the EM38 (Sheets and Hendrickx 1997). The Geonics EM38 manual instructs the user not to wear metallic objects such as watches or belt buckles because they can cause interference with the device and erroneous data can result. It is hypothesized that the high levels of iron in the soil at the Biological Field Station is the dominant factor controlling the response of the

EM38. Along the HR-Line iron alone controls almost 50% of the variation in the ECa when measured in the horizontal dipole mode. Iron was also found significant in three of the four regressions. As previously stated, the EM38 uses a magnetic inductance method to measure apparent electrical conductivity of the soil. If iron is present in high amounts, the EM38 will start to measure the magnetic field created by the iron and instead of the electric field in the soil. Therefore in soils with high iron content, it may be difficult to predict volumetric moisture content using the EM38.

Iron content does not fully justify why there is such a lack of correlation between apparent electrical conductivity and volumetric moisture content, but it does aid in identifying what is controlling the EM38 response. Iron content of soils remains relatively constant temporally. It is difficult to change the iron content of soils through natural processes in short periods of time.

2.4 Variability of ECa Reflected by Variograms

Variograms were constructed for all of the data to observe the spatial structure. Variograms relate properties spatially to one another. An attempt was made to relate the variograms of the apparent electrical conductivity to soil moisture.

Soil moisture varies and is highly dependant on precipitation. The Biological Field Station has a small weather center that records precipitation. Precipitation events are significant because they depict the amount of water available for retention by the soil. By studying the precipitation at the site, we can concur when soils are wetting, drying, or maintaining a relatively constant level of moisture. We use this information to attempt a relationship between the apparent electrical conductivity

measurements and the volumetric moisture content. It is hypothesized that wetter soils are more conductive than drier soils. The following is a chart of significant precipitation events at the site under investigation.

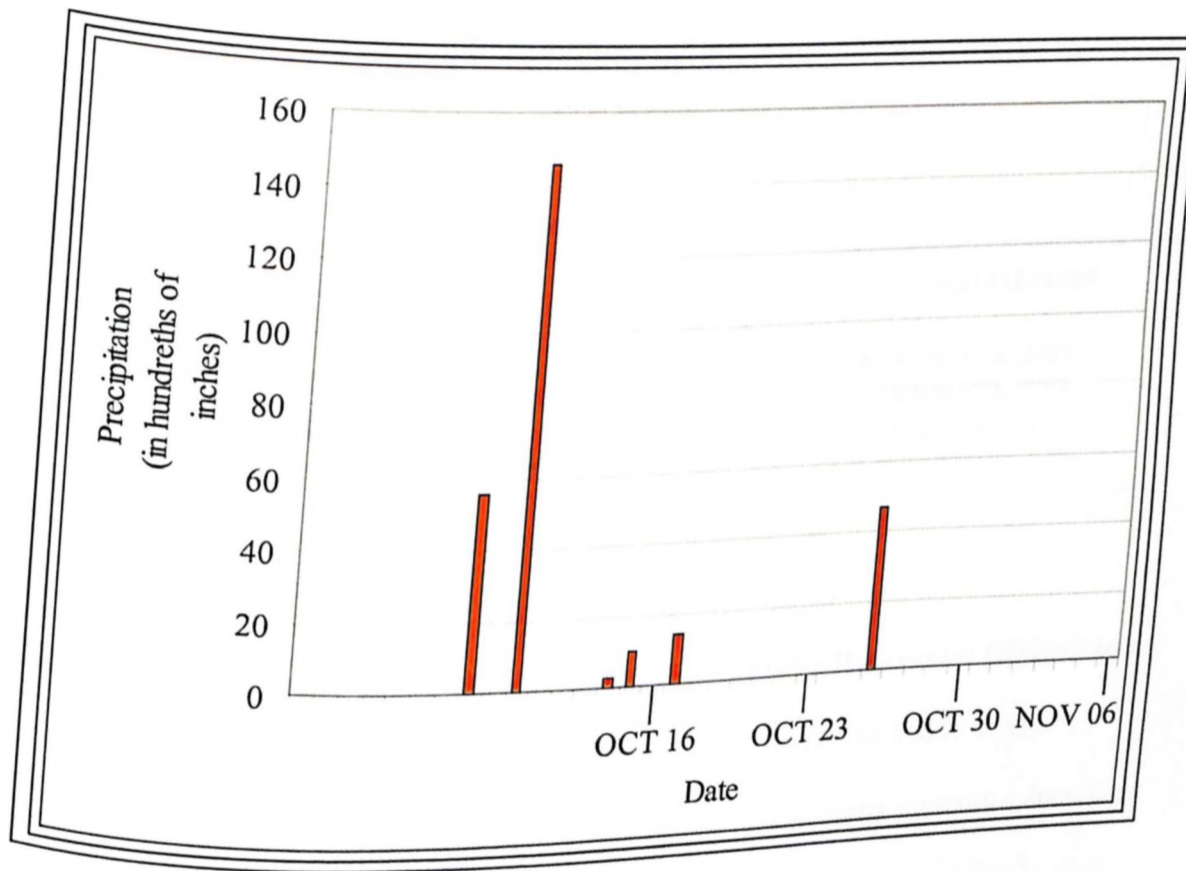


Figure 9 Significant Precipitation Events During Sampling

The four dates of EM measurements are shown at the bottom of the chart. Soil samples were taken on October 30 just after a significant rainfall event. For the purposes of this study, two significant rainfall events occurred that affected the data. One rainfall event prior to initial EM measurements and one just before the soil samples were taken are considered significant. Because the EM38 measures the apparent electrical conductivity with depth, we have to infer when this precipitation at the surface begins to affect the underlying sediments. The high volumetric moisture

contents measured from the soil cores suggest that the soil is near field capacity. Because the soil increases in sand content with depth, deeper sediments drain faster than shallow sediments. The EC_V is more likely to be influenced by this because it measures the deeper sediments than the EC_H . Figure 10 is the variograms of the T-line in the horizontal dipole mode.

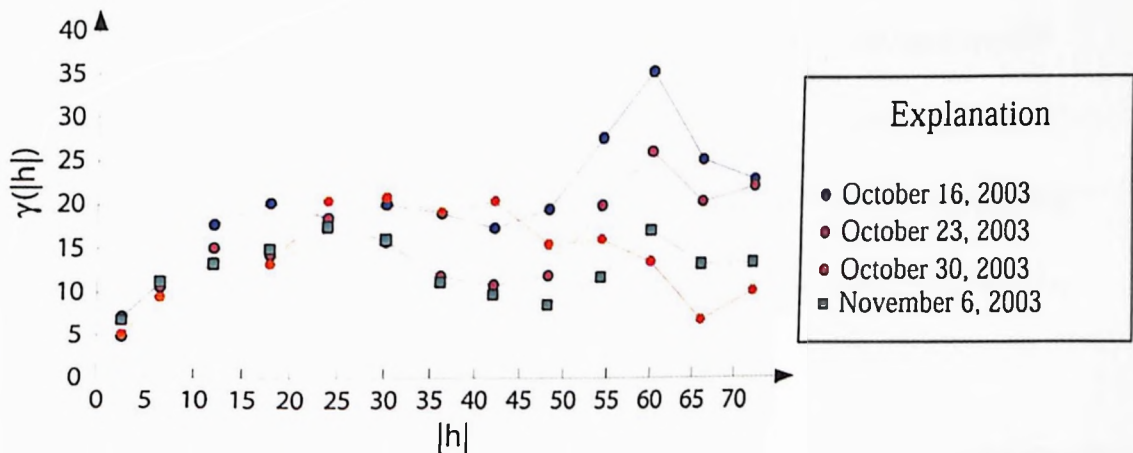


Figure 10 Variogram of the ECa Along the T-line in the Horizontal Dipole Mode

This variogram indicates that the measurements from the EM38 in the horizontal dipole mode have good spatial structures. Variograms spatially relate data so that relationships can be observed that are not apparent using basic statistics such as mean and standard deviation. Two populations can have the same mean and standard deviation but look totally different when viewed spatially. When good variograms such as these are obtained, they indicate that the ECa has spatial structure. They illustrate that our data is real and not randomly generated by the EM38. With these variograms, the correlation length varies between 20 and 25 meters. With spatially related measurements that are not random, it is inferred that the EM38 is measuring changes in ECa that change spatially.

All measurements show sill values of variance between 15 and 20 $(V\%/V)^2$. These are similar sill values to those observed by Western et al. (1998) when they observed soil moisture patterns in the Tarrawarra Catchment. They concur that the high variability is due to the high moisture content of the soils. The high moisture content means that the controls on soil moisture will be topographic rather than the water retention properties of the soil. The topography controls soil moisture by redistributing it laterally which increases the variability. Our field site is a hill (Figure 4) that slopes away from the intersection of the T and HR transects. Therefore we see a high variability of our soil moisture in the shallow sediments. Similar trends are observed in the T-line in the vertical dipole mode (Figure 11).

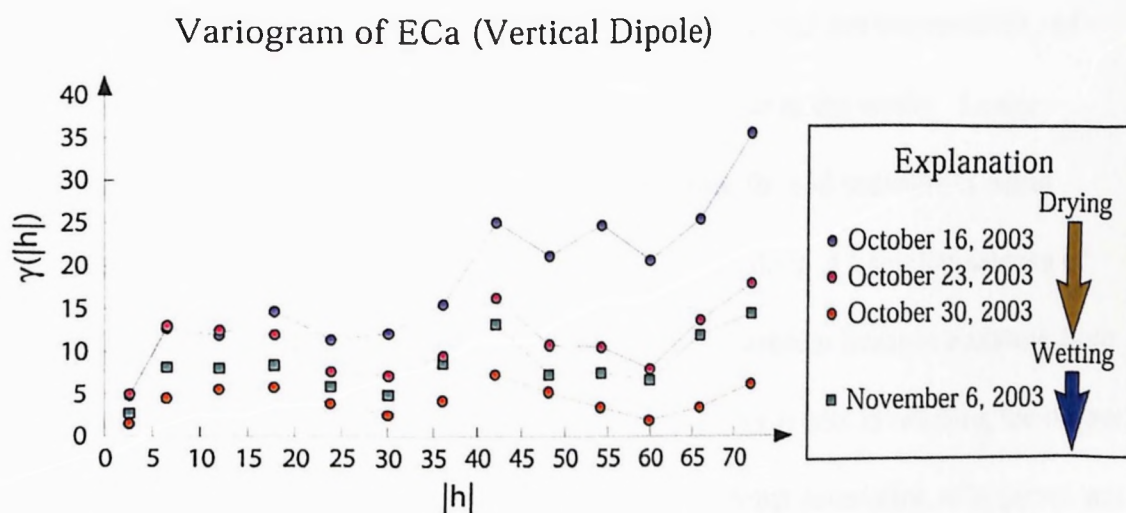


Figure 11 Variogram of the ECa Along the T-line in the Vertical Dipole Mode

Just like the horizontal dipole mode, we observe good variograms of ECa measured with the EM38. This too indicates that our data is not a random generation of ECa measurements, but rather data that has spatial structure. There are groups of high ECa and low ECa readings that are related to one another spatially. Here the correlation length, between 5 and 10 meters, is shorter than the horizontal mode.

Also apparent from this variogram is a similar trend observed on each measurement day. Peaks and valleys occur at the same spacing from week to week. This trend stays the same, but a decrease in total variability is seen throughout the first three measurement days. On the fourth measurement day, there is an increase in variability. In the vertical dipole mode the EM38 is measuring the deeper sediments. The sediments at the investigation site increase in sand content with depth. The increasing sand content means that the soils will drain faster than more shallow sediments. From the first three measurements days, the sediments are drying from the initial precipitation event prior to October 16. As the sediments dry they decrease in variability because the system becomes more homogeneous. This is consistent with the findings of Western et al. (1998) where they found that the variability of drier sediments in the summer was much less than those in the winter. Lower moisture means that the soil is more uniform because the soil moisture is being limited by the water retention properties of the soil so there is a smaller amount of lateral redistribution. On the fourth day, variability increases because moisture from the precipitation just prior to the October 30 measurement date is reaching the deeper sediments causing an increase in variability. While direct correlation of apparent soil electrical conductivity and volumetric moisture content was not apparent, increases and decreases in variability of the variograms of the ECa can be explained by precipitation events. With the EM38 data being normalized to a certain temperature, the only measured soil property able to change weekly in variability is soil moisture.

2.5 Negative Correlation Found in T Line

The largest coefficients of correlation obtained in the data analysis were between volumetric moisture content and apparent electrical conductivity over the T-Line with the EM38 in the horizontal dipole mode. Table 4 correlates volumetric moisture content to apparent electrical conductivity by depth of samples taken.

Depth (m)	Total		T Line		HR Line	
	Vertical ECa	Horizontal ECa	Vertical ECa	Horizontal ECa	Vertical ECa	Horizontal ECa
0.09 - 0.19	-0.2318	-0.0867	-0.2977	-0.1455	-0.1009	-0.0496
0.33 - 0.43	-0.0844	-0.2367	-0.1516	-0.4564	0.0246	0.1225
0.58 - 0.68	-0.0611	-0.2786	-0.1014	-0.6161	0.0847	0.2337
0.82 - 0.92	-0.1294	-0.3353	-0.1748	-0.5292	-0.0955	-0.0391
1.06 - 1.16	-0.0823	-0.3748	0.0847	-0.5413	-0.1137	

Table 4 Correlation Coefficients of ECa and Volumetric Moisture Content

A strong negative correlation exists along the T-Line in the horizontal dipole mode. An increase in moisture content decreases the conductivity of the soil. A positive correlation has been observed in previous studies (Sheets and Hendrickx 1995 and Reedy and Scanlon 2003). For there to be a negative correlation between soil moisture content and electrical conductivity, a property other than soil moisture must be influencing electrical conductivity. The level of compaction of the soil might influence the electrical conductivity of the soil more than the volumetric moisture content. Compaction greatly influences the conductivity of soils (Saarenketo 1998). In the four soil types he tested, an increase in compaction resulted in an increase in electrical conductivity. At the University of Mississippi Biological Field Station, the soils are near field capacity. As they increase in compaction and decrease in porosity, there is less space for water to occupy. Thus we see a negative correlation between volumetric moisture content and electrical conductivity. The soils are more compact resulting in a higher electrical conductivity, but there is less pore space for water and

thus there is a lower volumetric moisture content. There is a sharp rise in the electrical conductivity of soils as the water increases in volume such that it is beyond the electrical influences of the sediment particles and moves with gravity (Saarenketo 1998). There are three types of water in soils; hydroscopic, viscous, and free. Hydroscopic water is bound to the surfaces of the soil particles. Viscous water is not bound to the surfaces of the soil particles, but is attracted to them enough so that it will not respond to gravity. Free water is not bound to the surfaces of soil particles and can flow with gravity. The electrical conductivity of a soil increases dramatically when free water is present (Saarenketo 1998). At the UMBFS, the soils might be compacted so that the water present is 'squeezed' out from the hydroscopic layer to free water (Saarenketo 1998). Therefore with a decrease in volumetric moisture content, meaning a decrease in porosity, the water present is free water and not hydroscopic water thus there is an increase in electrical conductivity.

A negative correlation between volumetric moisture content and apparent electrical conductivity might also be observed in soils where the electrical conductivity is dominated by surface conductivity. It has been shown that for clays with the same moisture content, an increase in the degree of saturation will mean an increase in the electrical conductivity (McCarter 1984). Increasing the degree of saturation is a decrease in the air-void ratio. The soils at the UMBFS have between 10-15% clay (Figure 4). Thus it is possible for areas with smaller pore spaces and thus lower water contents, to conduct more electricity. This can possibly be the reason a negative correlation is observed with volumetric moisture content and apparent electrical conductivity. As the clay particles become more compact and

carry more electrical charge across the surfaces of the particles, there is less volumetric moisture content and a negative correlation exists.

3.0 Conclusions

The results of this field study show that at the UMBFS, there is no direct correlation between volumetric moisture content in the soil and apparent electrical conductivity measured from an EM38. Regressions between volumetric moisture contents at sample depths equivalent to the depth contribution to the EM38 also showed little correlation. The small physical soil samples taken may indicate that the scale to which the EM38 gains its response is too large to pick up small heterogeneities.

Regression analysis using the ten measured variables indicates soil physical properties control the EM38 response and apparent electrical conductivity. Iron content has the greatest influence on the EM38 response.

The results also indicate that overall variability may be controlled by wetting and drying events of the underlying soil. Also a negative correlation between volumetric moisture content and apparent electrical conductivity may be due to an increase in surface conductivity as porosity decreases.

Finally, the EM38 may not be able to detect volumetric moisture content in clay rich soils with significant heterogeneities, and high iron content.

BIBLIOGRAPHY

- Attaya, J. S., 1951. Lafayette County Geology: Mississippi State Geological Survey, Bulletin 71, 49 p.
- Cook, P.G., Walker, G.R., 1992. Depth Profiles of Electrical Conductivity from Linear Combinations of Electromagnetic Induction Measurements. Soil Science Society of America Journal Vol. 56. p. 1015-1022.
- Herrero, J., Aragues, A.A. Ba &R., 2003. Soil Salinity and Its Distribution Determined by Soil Sampling and Electromagnetic Techniques. Soil Use and Management Vol. 19. p 119-126.
- Huisman, J.A., Snepvangers, J.J.J.C., Bouten, W., Heuvelink, G. B. M., 2002. Mapping Spatial Variation in Surface Soil Water Content; Comparison of Ground-Penetrating Radar and Time Domain Reflectometry. Journal of Hydrology. Vol. 269. p. 194-207.
- Kachanoski, R.G., Gregorich, E.G., Van Wesenbeeck, I.J., 1988. Estimating Spatial Variations of Soil Water Content Using Noncontacting Electromagnetic Inductive Methods. Canadian Journal of Soil Science. Vol. 68. p. 715-722.
- Lesch, S.M., Strauss, D.J., Rhoades, J.D., 1995. Spatial Prediction of Soil Salinity Using Electromagnetic Induction Techniques I. Statistical Prediction Models: A Comparison of Multiple Linear Regression and Cokriging. Water Resources Research. Vol. 31. p. 373-386.
- McCarter, W.J. 1984. The Electrical Resistivity Characteristics of Compacted Clays. Geotechnique. Vol. 34 p. 263-267.

- McKenzie, R.C., George, R.J., Woods, S.A., Cannon, M.E., Bennett, D.L., 1997. Use of the Electromagnetic-Induction Meter (EM38) as a Tool in Managing Salinisation. *Hydrogeology Journal*. Vol. 5. p. 37-50.
- Qafoku, N.P., Sumner, M.E., 2002. Adsorption and Desorption of Indifferent Ions in Variable Charge Subsoils; the Possible Effect of Particle Interactions on the Counter-ion Charge Density. *Soil Science Society of America Journal*. Vol. 66 p. 1231-1239.
- Reedy, R.C., Scanlon, B.R., 2003. Soil Water Content Monitoring Using Electromagnetic Induction. *Journal of Geotechnical and Geoenvironmental Engineering*. Vol 129. p. 1028-1039.
- Rothe, A., Weis, W., Kreutzer, K., Mattheis, D., Hess, U., Ansorge, B., 1997. Changes in Soil Structure Caused by the Installation of Time Domain Reflectometry Probes and Their Influence on the Measurement of Soil Moisture. *Water Resources Research*. Vol. 33. p. 1585-1593.
- Saarenketo, T., 1998. Electrical Properties of Water in Clay and Silty Soils. *Ground Penetrating Radar Journal of Applied Geophysics*. Vol. 40. p. 73-88.
- Sheets, K.R., Hendrickx, J.M.H., 1995. Noninvasive Soil Water Content Measurement Using Electromagnetic Induction. *Water Resources Research*. Vol. 31. p. 2401-2409.
- Swann, C.T., Lutken, C.B., 2002. Suggested Water Quality Protection Practices for Unconfined Aquifers: A Case Study in the Meridian-Upper Wilcox Aquifer, North Mississippi, University of Mississippi Field Station Publication No. 13, 18 p.

Western, A.W., Bloeschl, G., Grayson, R.B., 1998. Geostatistical Characterization of Soil Moisture Patterns in the Tarrawarra Catchment. *Journal of Hydrology*. Vol. 205. p. 20-37.

Wollenhaupt, N.C., Richarsons, J.L., Foss, J.E., Doll, C. 1986. A Rapid Method for Estimating Weighted Soil Salinity from Apparent Soil Electrical Conductivity Measured with an Aboveground Electromagnetic Induction Meter. *Canadian Journal of Soil Science*. Vol. 66. p. 315-321.

APPENDIX A
ORIGINAL DATA

Boring ID	EC 10/16 Vertical (mS/m)	EC 10/16 Horizontal (mS/m)
T1	34.17	49.36
T2	34.17	56.95
T3	34.17	45.56
T4	37.97	49.36
T5	34.17	45.56
T6	30.38	41.77
T7	30.38	41.77
T8	34.17	45.56
T9	37.97	45.56
T10	34.17	41.77
T11	26.58	41.77
T12	22.78	37.97
T13	26.58	41.77
T14	30.38	45.56
T15	30.38	41.77
T16	30.38	45.56
T17	30.38	45.56
T18	30.38	41.77
T19	26.58	41.77
T20	26.58	34.17
T21	22.78	37.97
T22	26.58	37.97
T23	22.78	37.97
T24	22.78	34.17
T25	22.78	37.97
T26	30.38	41.77
T27	30.38	37.97
T28	26.58	37.97
T29	26.58	37.97
T30	26.58	41.77
T31	26.58	41.77
T32	26.58	41.77
T33	22.78	45.56
T34	22.78	49.36
T35	22.78	49.36
T36	26.58	41.77
T37	26.58	37.97
T38	26.58	37.97
T39	30.38	37.97
T40	30.38	37.97
T41	26.58	37.97
T42	22.78	37.97
T43	18.98	NA
H1	NA	NA
H2	NA	NA
H3	NA	NA
H4	NA	NA
H5	NA	NA
H6	NA	NA
H7	NA	NA
H8	NA	NA
H9	NA	NA
H10	NA	NA
H11	NA	NA
H12	NA	NA
H13	NA	NA
H14	NA	NA
H15	NA	NA
H16	NA	NA
H17	NA	NA
H18	NA	NA
H19	NA	NA
H20	NA	NA
H21	NA	NA
H22	NA	NA
H23	NA	NA
H24	NA	NA
H25	NA	NA
R1	NA	NA
R2	NA	NA
R3	NA	NA
R4	NA	NA
R5	NA	NA
R6	NA	NA
R7	NA	NA
R8	NA	NA
R9	NA	NA
R10	NA	NA

Boring ID	EC. 10/23 Vertical (mS/m)	EC. 10/23 Horizontal (mS/m)
T1	38.83	47.97
T2	40.21	54.83
T3	37.01	50.26
T4	42.03	50.26
T5	38.38	45.69
T6	36.55	45.69
T7	33.81	42.03
T8	39.29	43.40
T9	45.23	46.60
T10	42.03	47.52
T11	33.81	48.43
T12	32.90	46.60
T13	36.09	43.40
T14	37.46	47.52
T15	39.75	51.17
T16	41.12	50.26
T17	41.58	50.71
T18	42.49	53.91
T19	38.38	49.34
T20	37.46	45.69
T21	34.72	41.12
T22	36.55	44.77
T23	37.46	41.12
T24	36.09	38.83
T25	37.92	41.12
T26	42.03	42.49
T27	43.86	44.32
T28	42.49	45.23
T29	42.03	45.69
T30	41.12	43.40
T31	39.29	43.86
T32	40.21	43.40
T33	37.46	46.14
T34	38.83	46.14
T35	37.92	49.34
T36	40.66	48.89
T37	40.66	43.40
T38	41.12	39.75
T39	44.32	37.92
T40	47.97	44.32
T41	40.21	42.03
T42	36.55	42.49
T43	31.52	37.92
H1	NA	NA
H2	NA	NA
H3	NA	NA
H4	NA	NA
H5	NA	NA
H6	NA	NA
H7	NA	NA
H8	NA	NA
H9	NA	NA
H10	NA	NA
H11	NA	NA
H12	NA	NA
H13	NA	NA
H14	NA	NA
H15	NA	NA
H16	NA	NA
H17	NA	NA
H18	NA	NA
H19	NA	NA
H20	NA	NA
H21	NA	NA
H22	NA	NA
H23	NA	NA
H24	NA	NA
H25	NA	NA
R1	NA	NA
R2	NA	NA
R3	NA	NA
R4	NA	NA
R5	NA	NA
R6	NA	NA
R7	NA	NA
R8	NA	NA
R9	NA	NA
R10	NA	NA

Boring ID	EC 10/30 Vertical (mS/m)	EC 10/30 Horizontal (mS/m)
T1	20.81	30.87
T2	22.20	25.32
T3	21.85	24.62
T4	23.93	31.21
T5	23.58	20.81
T6	21.50	21.85
T7	19.77	21.50
T8	22.20	26.01
T9	24.62	30.17
T10	23.93	28.44
T11	19.42	26.70
T12	18.73	25.32
T13	20.46	24.97
T14	21.85	26.01
T15	24.28	29.48
T16	24.97	29.13
T17	24.28	30.17
T18	24.28	24.97
T19	20.81	24.28
T20	20.46	19.77
T21	18.73	17.34
T22	18.73	22.20
T23	19.42	18.03
T24	19.42	18.38
T25	19.77	20.46
T26	24.28	21.16
T27	24.28	25.32
T28	23.58	24.97
T29	23.93	26.70
T30	23.58	24.97
T31	22.54	24.97
T32	21.50	26.70
T33	20.12	27.75
T34	21.16	31.21
T35	21.16	30.52
T36	22.54	31.91
T37	22.89	26.36
T38	23.24	27.75
T39	24.97	24.97
T40	24.97	26.70
T41	23.58	27.75
T42	20.46	29.48
T43	17.34	23.58
H1	18.73	17.34
H2	18.38	13.18
H3	21.50	20.46
H4	20.81	22.20
H5	21.16	28.44
H6	22.89	21.50
H7	22.54	24.97
H8	23.24	23.58
H9	22.20	28.79
H10	20.46	27.05
H11	23.93	23.24
H12	22.54	31.21
H13	19.42	31.91
H14	14.91	25.66
H15	15.61	26.01
H16	15.61	24.97
H17	13.53	24.97
H18	13.18	24.28
H19	12.83	20.81
H20	14.57	24.97
H21	11.10	23.58
H22	11.10	21.16
H23	12.14	16.30
H24	12.49	13.87
H25	10.40	15.26
R1	27.75	20.81
R2	29.13	20.81
R3	30.52	31.91
R4	33.29	28.44
R5	34.33	29.13
R6	29.13	27.05
R7	31.21	21.85
R8	25.66	23.58
R9	24.28	20.81
R10	23.93	

Boring ID	EC 11/6 Vertical (mS/m)	EC 11/6 Horizontal (mS/m)
T1	15.69	
T2	18.83	43.04
T3	18.83	45.73
T4	22.42	40.80
T5	19.28	41.25
T6	17.93	38.56
T7	16.14	39.46
T8	18.83	36.32
T9	24.21	36.32
T10	22.42	42.59
T11	16.59	41.25
T12	14.80	37.66
T13	17.49	36.77
T14	18.83	34.97
T15	22.42	37.66
T16	22.42	42.59
T17	22.87	42.15
T18	26.00	40.80
T19	23.31	49.32
T20	25.56	45.73
T21	19.28	45.73
T22	21.07	40.35
T23	21.52	42.59
T24	17.93	41.25
T25	19.28	34.08
T26	22.42	36.32
T27	25.56	38.11
T28	23.31	38.11
T29	23.76	36.77
T30	21.97	40.35
T31	20.62	37.21
T32	23.31	40.35
T33	19.28	38.56
T34	20.62	41.25
T35	18.38	43.04
T36	20.62	43.94
T37	21.52	44.39
T38	22.42	37.66
T39	25.56	38.11
T40	26.45	35.87
T41	22.87	45.28
T42	18.38	39.46
T43	13.45	40.80
H1	17.49	32.73
H2	17.93	39.01
H3	19.73	36.77
H4	18.83	40.35
H5	20.62	36.77
H6	20.18	37.21
H7	20.62	37.66
H8	17.04	39.46
H9	17.93	40.35
H10	15.69	42.59
H11	17.04	40.80
H12	18.38	38.56
H13	15.69	40.35
H14	9.86	41.25
H15	11.66	34.52
H16	9.42	34.08
H17	8.07	33.63
H18	7.17	33.18
H19	6.73	29.59
H20	8.07	30.94
H21	4.93	33.63
H22	4.93	29.59
H23	5.83	26.45
H24	7.17	24.66
H25	5.38	20.18
R1	19.60	20.62
R2	21.32	25.56
R3	21.67	27.80
R4	24.08	28.25
R5	24.42	31.39
R6	19.95	31.83
R7	20.64	26.00
R8	17.54	26.90
R9	15.48	22.87
R10	13.76	20.18

Boring ID	Porosity	Bulk Density	% Sand	% Silt	% Clay	Average Volumetric Moisture Content	Average Graviometric Moisture Content	Fe	Al	Ca	K	Mg	Mn	Nb
T1	0.4141	1.5527	0.2188	0.7085	0.0718	0.3009	0.1937	16999.02	9005.86	1107.62	748.35	1383.79	384.16	174.55
T2	0.4051	1.5765	0.2197	0.7154	0.0649	0.3213	0.2040	19289.69	14061.88	985.41	1024.85	2035.67	404.08	188.88
T3	0.4027	1.5829	0.3496	0.5905	0.0599	0.3436	0.2179	20192.08	13871.16	1444.94	1040.28	2001.97	495.90	146.06
T4	0.4852	1.3643	0.2409	0.6964	0.0628	0.3319	0.2715	18206.46	9024.45	1409.87	724.82	1616.69	407.92	122.57
T5	0.4103	1.5828	0.2185	0.7198	0.0617	0.3527	0.2263	18933.19	8538.91	1330.86	720.93	1470.38	392.90	119.91
T6	0.3939	1.6061	0.2465	0.6958	0.0576	0.3827	0.2384	21164.01	14226.51	1084.22	993.71	1872.21	385.15	144.24
T7	0.4275	1.5170	0.2334	0.6931	0.0735	0.3705	0.2447	18282.85	13861.46	1106.61	1110.19	1797.05	310.24	253.30
T8	0.4191	1.5393	0.1878	0.7409	0.0713	0.3709	0.2411	17439.44	10657.26	1408.38	728.03	605.31	330.17	101.06
T9	0.3852	1.6291	0.2116	0.7251	0.0634	0.3661	0.2251	18597.01	10660.20	1220.95	858.96	1620.71	387.15	195.12
T10	0.4081	1.5685	0.2333	0.7001	0.0665	0.3736	0.2385	20429.94	12310.63	1096.68	902.76	1859.89	382.05	83.96
T11	0.3911	1.6197	0.2164	0.7176	0.0661	0.3911	0.2416	18428.79	11272.03	789.53	775.10	1813.21	334.67	77.72
T12	0.3891	1.6188	0.1536	0.7690	0.0774	0.3815	0.2364	20403.91	12104.00	815.01	797.82	1826.42	284.34	77.87
T13	0.4209	1.7121	0.1880	0.7377	0.0744	0.4209	0.2464	17360.33	8856.67	1035.59	741.05	1537.66	478.77	285.26
T14	0.3924	1.6101	0.1982	0.7316	0.0702	0.3731	0.2321	20110.63	11499.71	1621.66	929.50	1875.87	560.31	439.08
T15	0.3878	1.6680	0.2389	0.6996	0.0615	0.3878	0.2328	19780.46	11738.31	1462.08	932.60	1933.39	433.20	356.40
T16	0.3914	1.6378	0.2002	0.7290	0.0709	0.3914	0.2392	19340.12	10609.03	1538.94	783.74	1538.58	448.99	309.74
T17	0.3936	1.6069	0.2373	0.6938	0.0689	0.3918	0.2440	19324.79	11090.19	1285.51	884.93	1791.51	505.87	323.52
T18	0.4454	1.5873	0.2046	0.7259	0.0694	0.4454	0.2858	18968.84	10307.94	1442.27	834.24	1908.11	518.88	328.16
T19	0.4165	1.5464	0.1991	0.7200	0.0809	0.3705	0.2398	18379.21	10205.28	1697.05	807.59	1757.30	382.66	377.70
T20	0.4118	1.5588	0.1914	0.7456	0.0630	0.3653	0.2345	18900.31	10993.92	1053.97	844.03	1698.16	559.37	165.44
T21	0.4227	1.6625	0.1822	0.7561	0.0617	0.4227	0.2547	14137.29	6232.09	937.68	509.46	1139.43	321.89	117.19
T22	0.4414	1.8438	0.1953	0.7352	0.0695	0.4414	0.2420	13325.26	6111.41	830.72	469.11	1099.40	302.84	115.08
T23	0.4128	1.7496	0.1767	0.7467	0.0767	0.4128	0.2363	13212.48	5276.29	1012.36	437.84	1035.02	418.25	141.75
T24	0.4227	1.7284	0.2108	0.7212	0.0680	0.4227	0.2450	13433.13	5112.87	887.44	396.06	1022.53	346.37	165.39
T25	0.4056	1.7330	0.2278	0.6987	0.0736	0.4056	0.2348	14105.27	6092.59	1038.58	478.81	1161.24	372.99	128.74
T26	0.4025	1.7123	0.1666	0.7514	0.0820	0.4025	0.2357	18687.57	11566.14	1323.90	849.57	1701.21	511.81	76.64
T27	0.3982	1.6427	0.1789	0.7103	0.1108	0.3982	0.2424	17784.23	9571.73	1248.45	741.49	1564.81	546.09	96.11
T28	0.3868	1.6249	0.1772	0.7464	0.0765	0.3763	0.2319	18566.02	11883.46	1184.62	785.10	1724.14	381.42	71.92
T29	0.3994	1.6002	0.1609	0.7598	0.0793	0.3994	0.2503	20242.76	11561.01	1365.17	855.37	1838.66	442.86	124.03
T30	0.4087	1.5670	0.2501	0.6848	0.0651	0.3638	0.2327	18856.73	14488.34	3579.91	912.91	1892.76	394.64	146.61
T31	0.3874	1.6869	0.2459	0.6868	0.0674	0.3874	0.2298	18901.90	13731.04	1154.01	935.54	1726.34	383.22	136.13
T32	0.3887	1.6199	0.2390	0.6969	0.0641	0.3411	0.2108	21475.76	8990.09	1197.34	889.27	1407.84	343.17	160.88
T33	0.3913	1.6131	0.2792	0.6846	0.0562	0.3240	0.2020	17753.56	11383.75	946.53	712.86	1543.15	281.32	138.39
T34	0.4038	1.5801	0.2724	0.6694	0.0581	0.3105	0.1985	16981.40	9511.83	974.21	651.97	1441.85	306.07	143.20
T35	0.4299	1.5108	0.2848	0.6527	0.0625	0.3022	0.2019	17028.48	8783.11	840.36	645.93	1432.66	266.77	139.80
T36	0.3786	1.6467	0.2232	0.7046	0.0722	0.3310	0.2034	17521.68	12125.54	1005.28	752.60	1416.87	254.52	150.03
T37	0.3980	1.5952	0.2572	0.6824	0.0604	0.3092	0.1971	16804.05	8994.42	1491.86	642.36	1285.33	203.70	358.28
T38	0.3809	1.6405	0.2668	0.6686	0.0647	0.3268	0.2024	19596.91	14309.36	1368.99	925.01	1506.60	150.87	170.98
T39	0.4054	1.5757	0.3098	0.6352	0.0550	0.3317	0.2130	18574.62	13755.22	13300.27	742.04	1580.53	232.62	479.61
T40	0.4154	1.5492	0.2443	0.6921	0.0696	0.3397	0.2197	10759.95	5964.07	855.49	508.68	944.69	300.78	109.35
H1	0.4010	1.5873	0.2576	0.6766	0.0658	0.3768	0.2377							
H2	0.4207	1.5351	0.2758	0.6674	0.0568	0.3783	0.2479							
H3	0.4166	1.5459	0.3136	0.6200	0.0664	0.3731	0.2418							
H4	0.4054	1.5756	0.1889	0.7398	0.0713	0.3775	0.2402	19739.36	12504.77	1231.60	938.34	1874.11	562.90	184.47
H5	0.4125	1.5589	0.2111	0.7184	0.0705	0.3842	0.2467	21812.48	14807.45	1413.56	1147.58	2109.04	529.24	181.52
H6	0.4355	1.4859	0.3118	0.6352	0.0580	0.3909	0.2623	15150.53	9254.05	1182.57	785.54	1212.99	489.22	208.75
H7	0.4012	1.5869	0.3524	0.5897	0.0578	0.3722	0.2347	15906.06	10031.01	878.92	756.27	1396.40	295.63	158.51
H8	0.4131	1.5554	0.2548	0.6861	0.0591	0.3903	0.2511	20028.50	9950.12	1068.07	776.32	1680.66	384.93	113.68
H9	0.3814	1.6393	0.2523	0.6854	0.0624	0.3725	0.2290	21200.84	15946.61	1455.17	1104.45	2360.90	551.11	260.14
H10	0.4278	1.5164	0.3826	0.5688	0.0485	0.3321	0.2220	19818.11	13509.08	889.57	898.11	1880.54	381.67	134.97
R1	0.4161	1.5474	0.2252	0.7098	0.0652	0.3548	0.2283	19576.89	13063.86	2405.28	1008.35	2469.88	500.46	356.61
R2	0.4130	1.5556	0.2808	0.6416	0.0777	0.3561	0.2288	18834.44	13787.12	1675.58	1013.67	1788.53	483.46	281.75
R3	0.4119	1.5584	0.3639	0.5825	0.0538	0.3687	0.2367							
R4	0.4014	1.5852	0.2557	0.6483	0.0660	0.3845	0.2427	22814.49	18727.13	1887.02	1195.85	2367.82	454.78	346.42
R5	0.3956	1.6017	0.2683	0.6146	0.1171	0.3804	0.2377	19533.03	11242.90	1607.11	788.00	1758.30	381.02	336.83
R6	0.4079	1.5691	0.2911	0.6513	0.0576	0.3585	0.2292	18575.22	8241.73	1544.33	717.15	1885.82	310.37	312.39
R7	0.3915	1.6124	0.2897	0.6531	0.0572	0.3482	0.2164	18535.58	9418.34	1225.09	722.28	1881.82	431.88	311.35
R8	0.4065	1.5727	0.3008	0.6466	0.0528	0.3068	0.1942	17519.25	8495.88	1372.85	612.99	1543.73	326.09	312.71
R9	0.3721	1.6538	0.3084	0.6406	0.0510	0.2943	0.1776	20042.53	13020.88	1802.53	900.06	1955.21	467.31	335.65
R10	0.4472	1.4648	0.3127	0.6336	0.0537	0.2713	0.1858							

Boring ID	Sample Depth (m)	Volumetric Moisture Content
T1	0.09-0.19	0.336875865
T2	0.09-0.19	0.312056888
T3	0.09-0.19	0.300180773
T4	0.09-0.19	0.295436292
T5	0.09-0.19	0.32602772
T6	0.09-0.19	0.358645397
T7	0.09-0.19	0.346427153
T8	0.09-0.19	0.342507222
T9	0.09-0.19	0.349843774
T10	0.09-0.19	0.355123102
T11	0.09-0.19	0.380056366
T12	0.09-0.19	0.417501065
T13	0.09-0.19	0.439646149
T14	0.09-0.19	0.426844117
T15	0.09-0.19	0.360433053
T16	0.09-0.19	0.364114161
T17	0.09-0.19	0.36475837
T18	0.09-0.19	0.382805743
T19	0.09-0.19	0.336508147
T20	0.09-0.19	0.340524098
T21	0.09-0.19	0.385020167
T22	0.09-0.19	0.473836608
T23	0.09-0.19	0.349412802
T24	0.09-0.19	0.38133933
T25	0.09-0.19	0.382380414
T26	0.09-0.19	0.376960142
T27	0.09-0.19	0.378606884
T28	0.09-0.19	0.349494358
T29	0.09-0.19	0.380699826
T30	0.09-0.19	0.37270632
T31	0.09-0.19	0.39969434
T32	0.09-0.19	0.359226124
T33	0.09-0.19	0.345574182
T34	0.09-0.19	0.36094216
T35	0.09-0.19	0.402159033
T36	0.09-0.19	0.361296923
T37	0.09-0.19	0.367354378
T38	0.09-0.19	0.372059707
T39	0.09-0.19	0.377287652
T40	0.09-0.19	0.340879803
H1	0.09-0.19	0.368756424
H2	0.09-0.19	0.358726048
H3	0.09-0.19	0.359529099
H4	0.09-0.19	0.360010665
H5	0.09-0.19	0.362777085
H6	0.09-0.19	0.337865523
H7	0.09-0.19	0.352662684
H8	0.09-0.19	0.390441465
H9	0.09-0.19	0.380217323
H10	0.09-0.19	0.361686593
R1	0.09-0.19	0.319699183
R2	0.09-0.19	0.319699183
R3	0.09-0.19	0.295745688
R4	0.09-0.19	0.295745688
R5	0.09-0.19	0.361543708
R6	0.09-0.19	0.361543708
R7	0.09-0.19	0.371768228
R8	0.09-0.19	0.378848654
R9	0.09-0.19	0.378848654
R10	0.09-0.19	0.334040401
		0.358288736
		0.141453573
		0.335921271
		0.114464111

Boring ID	Sample Depth (m)	Volumetric Moisture Content
T1	0.33-0.43	0.277309772
T2	0.33-0.43	0.30361886
T3	0.33-0.43	0.336924491
T4	0.33-0.43	0.344168921
T5	0.33-0.43	0.363474797
T6	0.33-0.43	0.398542952
T7	0.33-0.43	0.365949804
T8	0.33-0.43	0.382443141
T9	0.33-0.43	0.361270134
T10	0.33-0.43	0.376211275
T11	0.33-0.43	0.393034362
T12	0.33-0.43	0.395844114
T13	0.33-0.43	0.433725391
T14	0.33-0.43	0.374323467
T15	0.33-0.43	0.396054426
T16	0.33-0.43	0.386202716
T17	0.33-0.43	0.381477906
T18	0.33-0.43	0.392384729
T19	0.33-0.43	0.370400362
T20	0.33-0.43	0.37617882
T21	0.33-0.43	0.378145167
T22	0.33-0.43	0.445097206
T23	0.33-0.43	0.41362394
T24	0.33-0.43	0.409716356
T25	0.33-0.43	0.414473526
T26	0.33-0.43	0.40030237
T27	0.33-0.43	0.415846105
T28	0.33-0.43	0.392935177
T29	0.33-0.43	0.412304326
T30	0.33-0.43	0.397515277
T31	0.33-0.43	0.392564595
T32	0.33-0.43	0.351878647
T33	0.33-0.43	0.349956194
T34	0.33-0.43	0.340137711
T35	0.33-0.43	
T36	0.33-0.43	0.348509772
T37	0.33-0.43	
T38	0.33-0.43	0.344139591
T39	0.33-0.43	0.350642108
T40	0.33-0.43	0.354537986
H1	0.33-0.43	0.371285866
H2	0.33-0.43	0.385138876
H3	0.33-0.43	0.391812018
H4	0.33-0.43	0.386828934
H5	0.33-0.43	0.387761478
H6	0.33-0.43	0.37170104
H7	0.33-0.43	0.393095321
H8	0.33-0.43	0.409074446
H9	0.33-0.43	0.387703381
H10	0.33-0.43	0.341273625
R1	0.33-0.43	0.362469788
R2	0.33-0.43	0.365472356
R3	0.33-0.43	0.387904508
R4	0.33-0.43	0.396360217
R5	0.33-0.43	0.395071374
R6	0.33-0.43	0.340065653
R7	0.33-0.43	0.372223189
R8	0.33-0.43	0.118748111
R9	0.33-0.43	
R10	0.33-0.43	0.110325909

Boring ID	Sample Depth (m)	Volumetric Moisture Content
T1	0.58-0.68	0.277013559
T2	0.58-0.68	0.327722857
T3	0.58-0.68	0.369742466
T4	0.58-0.68	0.33716529
T5	0.58-0.68	0.389981495
T6	0.58-0.68	0.397873847
T7	0.58-0.68	0.372570544
T8	0.58-0.68	0.398260112
T9	0.58-0.68	0.38382833
T10	0.58-0.68	0.372323364
T11	0.58-0.68	0.392326574
T12	0.58-0.68	0.393996092
T13	0.58-0.68	0.410935717
T14	0.58-0.68	0.374475769
T15	0.58-0.68	0.398373225
T16	0.58-0.68	0.400211824
T17	0.58-0.68	0.429149617
T18	0.58-0.68	0.4017509
T19	0.58-0.68	0.380265846
T20	0.58-0.68	0.380583658
T21	0.58-0.68	0.450776625
T22	0.58-0.68	0.437774891
T23	0.58-0.68	0.445294692
T24	0.58-0.68	0.446775931
T25	0.58-0.68	0.417514064
T26	0.58-0.68	0.425983467
T27	0.58-0.68	0.432027371
T28	0.58-0.68	0.404702106
T29	0.58-0.68	0.400511474
T30	0.58-0.68	0.395689253
T31	0.58-0.68	0.349871099
T32	0.58-0.68	0.342267495
T33	0.58-0.68	0.293465772
T34	0.58-0.68	0.256407235
T35	0.58-0.68	0.338042779
T36	0.58-0.68	0.286009182
T37	0.58-0.68	
T38	0.58-0.68	0.323590882
T39	0.58-0.68	0.37512384
T40	0.58-0.68	0.390803483
H1	0.58-0.68	0.357066231
H2	0.58-0.68	0.400183761
H3	0.58-0.68	0.405490958
H4	0.58-0.68	0.369088806
H5	0.58-0.68	0.381427074
H6	0.58-0.68	0.394711473
H7	0.58-0.68	0.404259836
H8	0.58-0.68	0.327272823
H9	0.58-0.68	0.385753792
H10	0.58-0.68	0.389100211
R1	0.58-0.68	0.388121866
R2	0.58-0.68	0.386452409
R3	0.58-0.68	0.395905653
R4	0.58-0.68	0.379760321
R5	0.58-0.68	0.354271103
R6	0.58-0.68	0.122200922
R7	0.58-0.68	0.125802573
R8	0.58-0.68	0.114763743
R9	0.58-0.68	
R10	0.58-0.68	

Boring ID	Sample Depth (m)	Volumetric Moisture Content
T1	0.82-0.92	0.312561562
T2	0.82-0.92	0.34189612
T3	0.82-0.92	0.367648229
T4	0.82-0.92	0.35079909
T5	0.82-0.92	0.331280094
T6	0.82-0.92	0.398581891
T7	0.82-0.92	0.397050196
T8	0.82-0.92	0.360425511
T9	0.82-0.92	0.380883604
T10	0.82-0.92	0.390690428
T11	0.82-0.92	0.398931404
T12	0.82-0.92	0.348111478
T13	0.82-0.92	0.428530993
T14	0.82-0.92	0.389541333
T15	0.82-0.92	0.396494686
T16	0.82-0.92	0.414944922
T17	0.82-0.92	0.406800557
T18	0.82-0.92	0.395002664
T19	0.82-0.92	0.364017578
T20	0.82-0.92	0.395544034
T21	0.82-0.92	0.409001156
T22	0.82-0.92	0.442986074
T23	0.82-0.92	0.452859093
T24	0.82-0.92	0.407910615
T25	0.82-0.92	0.406859988
T26	0.82-0.92	0.366122033
T27	0.82-0.92	0.377615238
T28	0.82-0.92	0.400062158
T29	0.82-0.92	0.280481466
T30	0.82-0.92	0.361568448
T31	0.82-0.92	0.303264414
T32	0.82-0.92	0.302282802
T33	0.82-0.92	0.275819804
T34	0.82-0.92	0.265887156
T35	0.82-0.92	0.308460834
T36	0.82-0.92	0.297351458
T37	0.82-0.92	0.291105036
T38	0.82-0.92	0.311069376
T39	0.82-0.92	
T40	0.82-0.92	0.392213742
H1	0.82-0.92	0.382376486
H2	0.82-0.92	0.383903169
H3	0.82-0.92	
H4	0.82-0.92	0.380869744
H5	0.82-0.92	0.485078176
H6	0.82-0.92	0.37412589
H7	0.82-0.92	0.366836716
H8	0.82-0.92	0.361949206
H9	0.82-0.92	0.31932942
H10	0.82-0.92	0.365447005
R1	0.82-0.92	0.374008384
R2	0.82-0.92	0.347136649
R3	0.82-0.92	0.383376923
R4	0.82-0.92	0.3519189
R5	0.82-0.92	0.381404619
R6	0.82-0.92	0.341372999
R7	0.82-0.92	0.11723633
R8	0.82-0.92	0.272392177
R9	0.82-0.92	0.111380866
R10	0.82-0.92	

Boring ID	Sample Depth (m)	Volumetric Moisture Content
T1	1.06-1.16	
T2	1.06-1.16	
T3	1.06-1.16	
T4	1.06-1.16	
T5	1.06-1.16	
T6	1.06-1.16	
T7	1.06-1.16	0.360003194
T8	1.06-1.16	
T9	1.06-1.16	
T10	1.06-1.16	0.35468735
T11	1.06-1.16	
T12	1.06-1.16	
T13	1.06-1.16	0.351929833
T14	1.06-1.16	0.391626742
T15	1.06-1.16	0.300422765
T16	1.06-1.16	
T17	1.06-1.16	
T18	1.06-1.16	
T19	1.06-1.16	0.64345773
T20	1.06-1.16	
T21	1.06-1.16	
T22	1.06-1.16	0.504001527
T23	1.06-1.16	
T24	1.06-1.16	
T25	1.06-1.16	
T26	1.06-1.16	
T27	1.06-1.16	
T28	1.06-1.16	
T29	1.06-1.16	0.385041322
T30	1.06-1.16	
T31	1.06-1.16	0.367666178
T32	1.06-1.16	
T33	1.06-1.16	
T34	1.06-1.16	0.279884189
T35	1.06-1.16	0.281931369
T36	1.06-1.16	0.28437917
T37	1.06-1.16	0.29852211
T38	1.06-1.16	0.286189341
T39	1.06-1.16	0.299714416
T40	1.06-1.16	0.287964862
H1	1.06-1.16	
H2	1.06-1.16	
H3	1.06-1.16	
H4	1.06-1.16	
H5	1.06-1.16	0.363063836
H6	1.06-1.16	
H7	1.06-1.16	
H8	1.06-1.16	0.359763095
H9	1.06-1.16	
H10	1.06-1.16	0.328522312
R1	1.06-1.16	0.310921064
R2	1.06-1.16	0.340412772
R3	1.06-1.16	
R4	1.06-1.16	
R5	1.06-1.16	
R6	1.06-1.16	0.357454636
R7	1.06-1.16	0.172438505
R8	1.06-1.16	0.232077941
R9	1.06-1.16	
R10	1.06-1.16	

HR Line Horizontal Dipole Mode Best Reduced Regression Model

SUMMARY OUTPUT

<i>Regression Statistics</i>	
Multiple R	0.668998023
R Square	0.447558354
Adjusted R Square	0.408098237
Standard Error	3.041405001
Observations	16

ANOVA

	<i>df</i>	<i>SS</i>	<i>MS</i>	<i>F</i>	<i>Significance F</i>
Regression	1	104.9155363	104.9155	11.34204	0.004598251
Residual	14	129.5020213	9.250144		
Total	15	234.4175576			

	<i>Coefficients</i>	<i>Standard Error</i>	<i>t Stat</i>	<i>P-value</i>	<i>Lower 95%</i>	<i>Upper 95%</i>	<i>Lower 95.0%</i>	<i>Upper 95.0%</i>
Intercept	8.101324635	5.174574238	1.565602	0.13976	-2.997033273	19.19968254	-2.997033273	19.19968254
Fe	0.000917367	0.000272394	3.367795	0.004598	0.00033314	0.001501594	0.00033314	0.001501594

HR Line Vertical Mode Best Reduced Regression Model

SUMMARY OUTPUT

Regression Statistics	
Multiple R	0.946595973
R Square	0.896043936
Adjusted R Square	0.826739894
Standard Error	2.004965128
Observations	16

ANOVA

	df	SS	MS	F	Significance F
Regression	6	311.8427385	51.97379	12.92917276	0.000563623
Residual	9	36.17896647	4.019885		
Total	15	348.021705			

	Coefficients	Standard Error	t Stat	P-value	Lower 95%	Upper 95%	Lower 95.0%	Upper 95.0%
Intercept	28.65026734	8.660863664	3.308015	0.009112699	9.058032612	48.24250208	9.058032612	48.24250208
% Silt	-0.463345186	0.149107919	-3.107449	0.012570485	-0.800650732	-0.12603964	-0.800650732	-0.12603964
% Clay	1.268218677	0.310969593	4.078272	0.002765158	0.564756586	1.971680768	0.564756586	1.971680768
Fe	0.001140027	0.000370613	3.076057	0.013223929	0.000301642	0.001978412	0.000301642	0.001978412
Al	-0.003038856	0.001056188	-2.877193	0.018261355	-0.005428119	-0.000649593	-0.005428119	-0.000649593
K	0.028823908	0.014697097	1.961197	0.081487426	-0.004423236	0.062071051	-0.004423236	0.062071051
Na	0.030683257	0.006462849	4.747636	0.001047656	0.016063276	0.045303238	0.016063276	0.045303238

T Line Horizontal Dipole Mode Best Reduced Regression Model

SUMMARY OUTPUT

<i>Regression Statistics</i>	
Multiple R	0.612296693
R Square	0.37490724
Adjusted R Square	0.340179864
Standard Error	3.160151545
Observations	39

ANOVA

	<i>df</i>	<i>SS</i>	<i>MS</i>	<i>F</i>	<i>Significance F</i>
Regression	2	215.6243	107.8121	10.79573	0.000212325
Residual	36	359.5161	9.986558		
Total	38	575.1404			

	<i>Coefficients</i>	<i>Standard Error</i>	<i>t Stat</i>	<i>P-value</i>	<i>Lower 95%</i>	<i>Upper 95%</i>	<i>Lower 95.0%</i>	<i>Upper 95.0%</i>
Intercept	37.83412884	7.382557	5.1248	1.03E-05	22.86160955	52.80664814	22.86160955	52.80664814
Vol W.C.	-53.79569789	13.72951	-3.918253	0.000382	-81.64043469	-25.95096108	-81.64043469	-25.95096108
Fe	0.000419626	0.000245	1.712687	0.095372	-7.72779E-05	0.000916529	-7.72779E-05	0.000916529

T Line Vertical Dipole Mode Best Reduced Regression Model

SUMMARY OUTPUT

<i>Regression Statistics</i>	
Multiple R	0.483189235
R Square	0.233471837
Adjusted R Square	0.167769423
Standard Error	1.84549338
Observations	39

ANOVA

	df	SS	MS	F	Significance F
Regression	3	36.30775629	12.10259	3.553474	0.024039851
Residual	35	119.2046035	3.405846		
Total	38	155.5123598			

	Coefficients	Standard Error	t Stat	P-value	Lower 95%	Upper 95%	Lower 95.0%	Upper 95.0%
Intercept	19.90934595	1.579670193	12.60348	1.44E-14	16.70244499	23.11624692	16.70244499	23.11624692
Na	0.005713385	0.002871591	1.989623	0.054491	-0.000116256	0.011543025	-0.000116256	0.011543025
Mg	-0.002880791	0.001599485	-1.801074	0.080313	-0.006127919	0.000366336	-0.006127919	0.000366336
K	0.007297615	0.003014426	2.420897	0.020807	0.001178004	0.013417226	0.001178004	0.013417226